

Materials at High Temperatures

Impression Creep Test of a P91 Steel: A Round Robin Programme

--Manuscript Draft--

Manuscript Number:	MHT574R1	
Full Title:	Impression Creep Test of a P91 Steel: A Round Robin Programme	
Article Type:	Research Article	
Keywords:	Impression Creep Test; P91; Round Robin Programme	
Corresponding Author:	Charles Dyson University of Nottingham Nottingham, Nottinghamshire UNITED KINGDOM	
Corresponding Author Secondary Information:		
Corresponding Author's Institution:	University of Nottingham	
Corresponding Author's Secondary Institution:		
First Author:	Steve J Brett	
First Author Secondary Information:		
Order of Authors:	Steve J Brett	
	Charles Dyson	
	Daniel Purdy	
	John Shingledecker	
	Juhani Rantala	
	Jack Eaton-Mckay	
	Wei Sun	
Order of Authors Secondary Information:		
Abstract:	<p>The process of standardisation of small specimen creep testing techniques, specifically the impression creep test requires the repeatability of the test method. In this study it is accomplished through a round robin programme involving four different labs which have slightly different test set-ups adhering to predefined recommendations stated in previous work. The labs all conducted the same stepped stress test on a reference heat of grade 91 power plant steel and the displacement traces of the tests are analysed to outline the effects of different test set-ups and their efficacies. Main differences are in temperature control and loading application and control.</p>	
Additional Information:		
Question	Response	
Funding Information:	Engineering and Physical Sciences Research Council (EP/G037345/1)	Mr Charles Dyson
	BF2RA (20)	Mr Charles Dyson

Impression Creep Test of a P91 Steel: A Round Robin Programme

S.J. Brett¹, C.N.C Dyson^{1*}, D. Purdy², J. Shingledecker², J. Rantala³, J. Eaton-Mckay⁴, W. Sun¹

¹ *Faculty of Engineering, University of Nottingham NG7 2RD, UK*

² *Electric Power Research Institute, Palo Alto, California, USA*

³ *VTT Technical Research Centre FI-02044, Espoo, Finland*

⁴ *AMEC FW, Warrington WA3 6GA, UK*

*Corresponding author: Tel:+44 115 846 7683 email: ezxcd3@nottingham.ac.uk

Impression Creep Test of a P91 Steel: A Round Robin Programme

Abstract:

The process of standardisation of small specimen creep testing techniques, specifically the impression creep test requires the repeatability of the test method. In this study it is accomplished through a round robin programme involving four different labs which have slightly different test set-ups adhering to predefined recommendations stated in previous work. The labs all conducted the same stepped stress test on a reference heat of grade 91 power plant steel and the displacement traces of the tests are analysed to outline the effects of different test set-ups and their efficacies. Main differences are in temperature control and loading application and control.

Keywords: Impression Creep Test; P91; Round Robin Programme

INTRODUCTION

The need for more detailed information in the condition monitoring of power plant components is an ongoing concern which includes high temperature headers, main steam lines, and valve bodies. The use of small specimen creep test methods provides a method to obtain mechanical data from components. The impression creep test method is such a technique, originally performed using a cylindrical indenter [1], and later using a rectangular indenter loading a square specimen from which a mechanics based interpretation technique was developed [2]. It is capable of providing data from in-service components in the form of constant-load displacement rates (converted to the corresponding uniaxial secondary creep strain rates), where specimens are machined from component surface scoop samples. In this instance, strength ranking of components may be conducted and with further development aid in remnant life assessment strategies. In the latter case, conversion of the results may be needed. While in some cases material from the surface of high temperature components may contain the greatest damage [3] in other cases temperature and stress state dependant peak

damage may be present below the surface. In scenarios where material is limited, such as weldments where the separation between metallurgical zones may be small, full-size uniaxial creep testing may not be feasible and so local material characterization may only be possible with small specimen creep tests. In addition to the above requirement, small specimen creep test techniques may be of use in novel alloy development [4] where material quantities and test times are scarce.

The present work is an evaluation of the state of the art procedures involved in testing and is in reference to prior requirements as outlined by Hyde et al [5] who have extensive experience and have conducted hundreds of tests. It has been identified that load stability and control, temperature measurement and control, and displacement measurement are the key variable features in rig design which have a significant impact on test results, particularly displacement signal stability.

IMPRESSION CREEP TEST AND BASIC REQUIREMENTS

Impression Creep Test Using a Rectangular Indenter

Test Set-up

The impression creep testing technique described herein uses rectangular indenters and involves the application of a steady load to a flat-ended indenter, placed on the surface of a specimen, at elevated temperature. The dimensions used across labs in this study are illustrated in Figure 1. $b=w=10$ mm, $h=2.5$ and $d=1$.

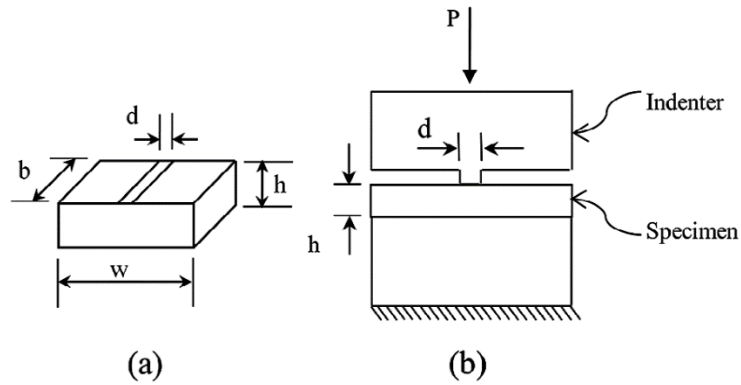


Figure 1: Indenter and specimen dimensions [6]

Conversion Relationships

The displacement-time record obtained from such a test is related to the creep properties of a relatively small volume of material in the immediate vicinity of the indenter. For the rectangular type of indenter, Hyde et al [7] used a reference stress approach to convert the mean pressure under the indenter, \bar{p} , to the corresponding uniaxial stress, σ , i.e.

$$\sigma = \eta \bar{p} \quad (1)$$

and to convert the impression load-direction creep displacement, Δ^c , to the corresponding uniaxial creep strain, ϵ^c , i.e.

$$\epsilon^c = \frac{\Delta^c}{\beta d} \quad (2)$$

where η and β are the conversion parameters (reference parameters) and d is the width of the rectangular indenter, Figure 1(a). Therefore, the secondary creep properties can be obtained from impression creep test data using such conversion relationships. The technique can

produce accurate results when the impression creep deformation occurring during the tests is small, compared with the indenter width or the specimen thickness. This may be done by limiting the secondary creep phase (which has a decreasing displacement rate) by allowing for a secondary creep trace that is approximately linear giving a minimum of a 100h for creep rate calculation, the test lengths are material and stress dependant. The conversion factors however are material independent. They depend on dimension ratios of indenter and specimens if the effect of the indenter deformation is neglected. η and β have been determined previously for a practical range of dimensions [2], [7].

Values for η and β are 0.430 and 2.180 [7] respectively for a standard sized specimen, if specimen dimensions are for some reason changed e.g. not enough material could be provided, ref [7] provides details on how to calculate the new values of the parameters.

Basic Requirements

Indenter and Specimen

The indenter must be made of material of significantly higher creep strength than the test material. In the case of fossil power plant pipework (CrMoV, P91) this means the use of nickel superalloys (Waspaloy or Nimonic) or ceramic indenters (Al_2O_3). This is so that creep occurs predominantly in the specimen; i.e. the creep strain rate present in the indenter must be negligible in comparison with the test specimen for the prescribed test conditions. The width of the indenter should also be greater than that of the specimen in order to make sure the whole length of the specimen is indented. A further requirement is that the indenter should be ground so as to be parallel with the flat surface of the specimen. Periodic checks between tests must be made on the indenter to make sure that it is flat, including the effects of oxide growth, if not the indenter may be ground so as to be made flat again, polishing of the surfaces to a recommended 200grit with a tolerance of $\pm 0.02mm$.

As shown in Figure 1(b), the specimen and indenter dimensions are defined by three ratios; w/d , w/b and h/d . d is the indenter width, w , b and h are the width, length and height of the specimen respectively. The recommended standard dimensions are $w \times b \times h = 10 \times 10 \times 2.5 \text{ mm}$ and $d = 1.0 \text{ mm}$. If material is scarce the height of the specimen can be reduced, as long as conversion requirements are corrected. Or, the standard specimen dimensions can be reduced proportionally e.g. $w \times b \times h = 8 \times 8 \times 2 \text{ mm}$ and $d = 0.8 \text{ mm}$ [7].

Loading, Measurement and Control

Indenter and Specimen Alignment and Load Application

Marking grooves into the specimen before alignment is recommended as guidance for where the indenter blade should sit. This allows for accurate alignment of the indenter to the specimen when placed on the lower loading bar, see Figure 1. Once aligned the specimen must be held in place by the indenter with a load around 10% of the test load so as to secure the specimen before heating. Once the furnace has reached the test temperature the full load may be applied. The applied load should be known to an accuracy of $\pm 1\%$ to agree with requirements in uniaxial creep testing BS EN ISO 204 [8]. In cases where servo mechanical loading is applied there is a requirement for active **control**.

Displacement Measurement

Displacement measurement can be conducted through the use of water-cooled linear variable displacement transducers (LVDTs) which are connected to the bottom of two extensometers. However, strain gauges or other more advanced methods may be used as long as measuring ranges lie within $\pm 0.2 \text{ mm}$ with an accuracy of 0.5%.

The deformations must be monitored and are recommended to be recorded through signal

conditioning and data logging software. The final displacement recorded by the data logger can be compared to an alternative measurement of the indentation depth for validation.

Temperature Control and Test Environment

The impression creep tests can be performed in air if the test temperatures are within the normal range of operating temperature for the material. Given the compressive contact between the sample and the indenter, oxidation effects on the surface are expected to be minimal even at long test durations.

In the Nottingham creep laboratory, three 0.5mm dia. K type thermocouples are used to control the temperature; however there is no restriction to the use of S type thermocouples. The middle one is close to the specimen and the upper and lower thermocouples are about 25mm away from the specimen, near to the extensometer ridges. These positions may not always be held at the specified temperature due to the heat balance in the furnace. However, experience of many tests, with the temperatures checked by calibrated thermocouples and visual output, has produced a high degree of confidence in using such methods. However, increasing the proximity of the thermocouples to the specimen would not be discouraged. Platinum resistance probes could be used in order to obtain a higher level of accuracy of temperature control or measurement.

BS EN ISO 204 [8] recommends a soak up period of 1 hour for full size uniaxial tests; the same recommendations are then passed on to the impression creep test method before full load is applied.

ROUND ROBIN IMPRESSION CREEP TEST PROGRAMME

Background and Motivation

The testing provides confidence that impression creep is capable of becoming a standardized test technique. In addition, the RR testing is required to show that there is sufficient expertise available to standards organisation bodies when the official standards are ready to be drafted and implemented. It is the aim that a deeper understanding of the test method may be achieved through the use of different set-ups that meet the minimum requirements.

Material and Test Conditions

A variant of P91 power plant steel of the same heat was tested, the material is referred to as BAR257 and has a hardness toward the soft end of the normal range of P91 i.e. 204HV. Its rupture strength shown to be [9], [10] close to 20% below the mean strength value for P91 [11]. The tests done in this Round Robin were stepped stress tests, the load is increased once a sufficiently low secondary creep strain rate is achieved (refer to sect 2.1.2). For this particular series of tests, five stress levels were performed on the same specimen, all at 600°C. No previous comparison of this type has been made across all testing laboratories. Loads and their converted stresses can be seen in table 1. Equation (1) is used to make the conversion calculations with $\eta = 0.430$ as the conversion constant. The specimen and indenter dimensions used are those taken from the Basic requirements in Section 2. Nottingham's results can be seen in Figure 2.

Table 1: Impression Creep Stresses

Stress (MPa)	89	98	104	118	134
--------------	----	----	-----	-----	-----

Equipment Specifications

Test Rig Descriptions

Experience at Nottingham has given rise to minimum specifications [5] pertaining to load delivery and sensitivity and the same for temperature. However, there is still scope for variations in rig design as described in table 2 for the different labs. The main purpose of this exercise is to highlight the effects that variations in design have on the indentation traces.

Materials used for the indenters can be made of nickel based super alloys however ceramic indenters may be used provided the sample polishing is increased to a higher level, allowing for less noise in the initial stages of creep. However lower coefficients of thermal expansion would result in increased strain rates in comparison to nickel alloy counterparts which have a similar thermal expansion to P91. It is therefore useful to not only find an indenter of higher creep strength but one with similar thermal expansion properties.

Loading Application

There are two possible loading methods described by the rigs in this programme, 'normal' which involves the indenter blade approaching from above the specimen which is resting on a mount and 'reverse', where the indenter blade is facing upwards and the specimen is loaded onto the blade.

Table 2: Test Rig Specifications

Organization	Loading Mechanism	Load Accuracy	Indenter Contact Correction	Specimen – indenter Orientation	Heat Delivery	Temperature Control (°C)	Temperature Measurement
AMEC	Dead-weight	10kN ±0.05N	Not required	Normal	Coils built into furnace wall	±0.5	Two k-type thermocouples
EPRI	Servo-mechanical	25kN ±1.25N	None	Normal	Coils built into furnace wall	±0.5	Three k-type thermocouples
NOTTS	Servo-mechanical	25kN ±1.25N	None	Normal	Coils built into furnace wall	±0.5	Three k-type thermocouples
VTT	Servo-mechanical	10kN ±0.05N	Floating indenter system	Reverse	Two flat coils on each loading bar	±0.3	Two R-type thermocouples

Test Results

Converted Minimum Creep Strain Rates

Generally there tends to be good agreement between the labs for the converted average impression creep strain rates (Figure 3). At each stress level within the stepped stress test as in Figure 2 (raw data from each lab is in the appendix) the final 100h of the test are used to calculate the strain rate using a linear regression through the data. Not all step lengths were the same between laboratories, this did not have a marked effect on the results as the 100h window required for calculating strain rates was present across all test data. Other methods were used which yielded results that tended to cluster around the same mean regression through the data points. These included firstly obtaining a plot of the strain rate with time, which is done by taking the slope forward and backward of each data point by either 25h or 50h. Taking the average of the resulting strain rates gave comparable results to those seen in Figure 3 and so the earlier method was used for the plot mainly due to ease of calculation. Figure 3 shows the impression strain rates for each lab compared to the minimum creep strain rate predicted for Grade 91 at mean and mean-20% rupture life values taken from the literature [11] and the Impression Monkman-Grant relationship [12]. The uniaxial formulation of the Monkman-Grant relationship [13] is,

$$C = \dot{\epsilon}_{min}^C * t_f \quad (3)$$

where C and m are material constants, $\dot{\epsilon}_{min}^C$ is the minimum creep strain rate (h^{-1}), the equation can be modified to:

$$ICR = 0.004575 * t_f^{-0.7391} \quad (4)$$

ICR is the impression creep strain rate (mmh^{-1}) and t_f (hrs) is the time to rupture in the conventional uniaxial test. Bar 257 falls in the normal-weak range for P91 and based on the results agrees at the lower stress levels. However at higher stress levels the strain rates deviate. Impression Monkman Grant curves deviate slightly from normal uniaxial curves.

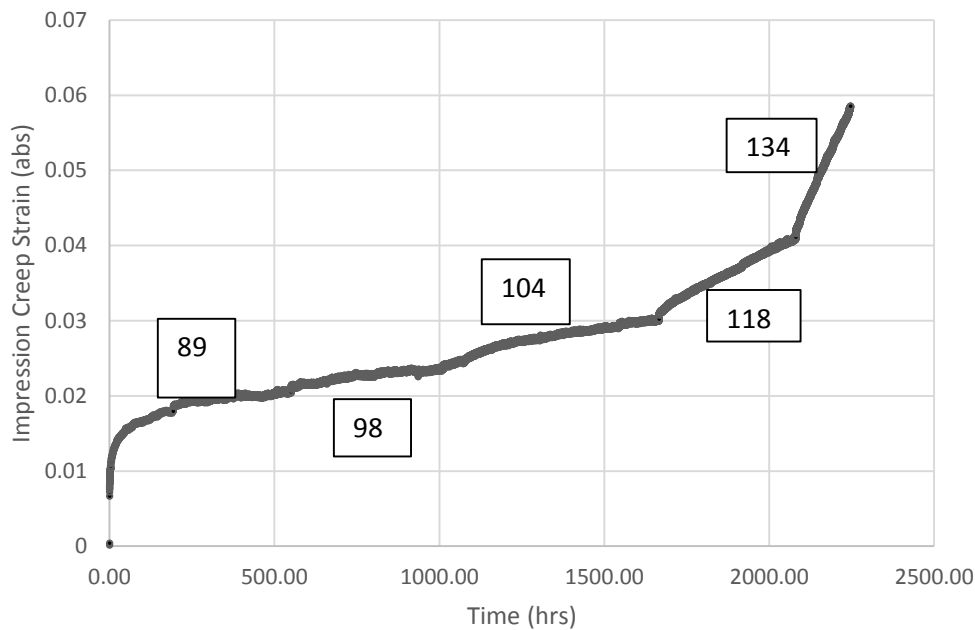


Figure 2: Nottingham stepped stress test results BAR 257 along with loads in MPa at each step

Displacement Rate Variation

For the purposes of the present paper the displacement rate variation will be described as the maximum amplitude in fluctuation of the strain rate signals for each stress level in the stepped stress test. The method used to determine the plot of the strain rate is mentioned above. At each point the strain rate is calculated for points 50h forwards and backwards of that point within the stress level and will be referred to as the 100h strain rate from now on, an example plot for all labs is shown in Figure 5. The maximum amplitude in the signal is determined by detrending the signal and then taking the Fourier transform of the signal to

identify the most prominent amplitude. This is then taken for each stress level and each lab, the averages across stress levels for each lab are compared in Figure 4.

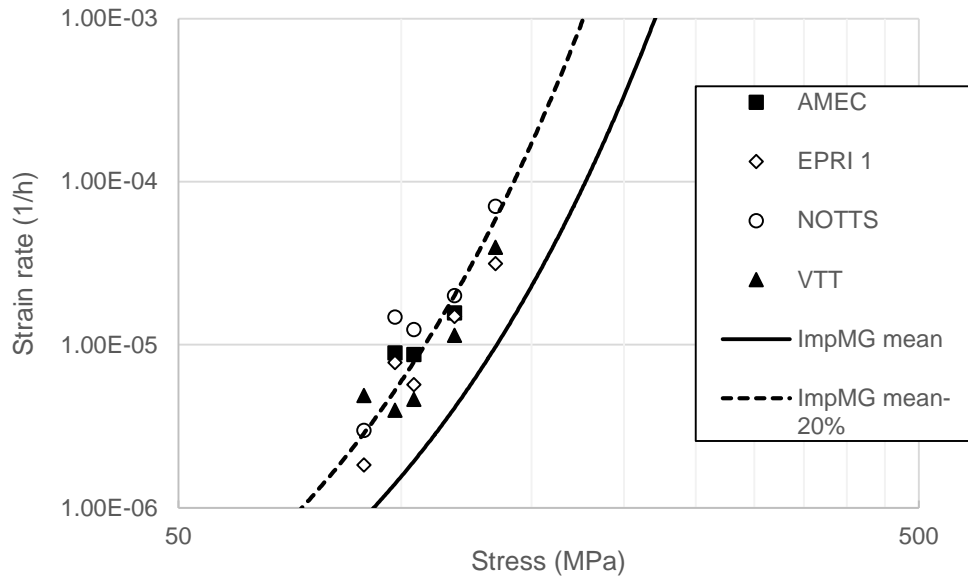


Figure 3: Converted impression strain rates from all labs against the converted strain rate predicted using the ECCC grade 91 mean and mean -20% rupture life [11] and the Impression Monkman Grant relationship

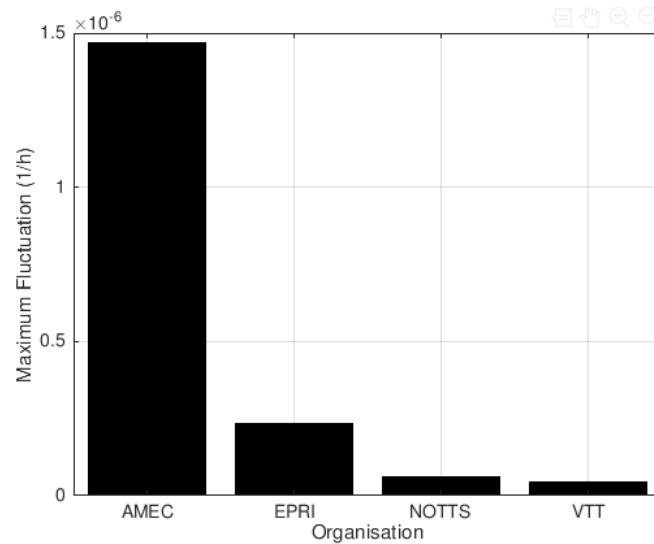


Figure 4: Maximum strain rate fluctuation averaged from all stress levels

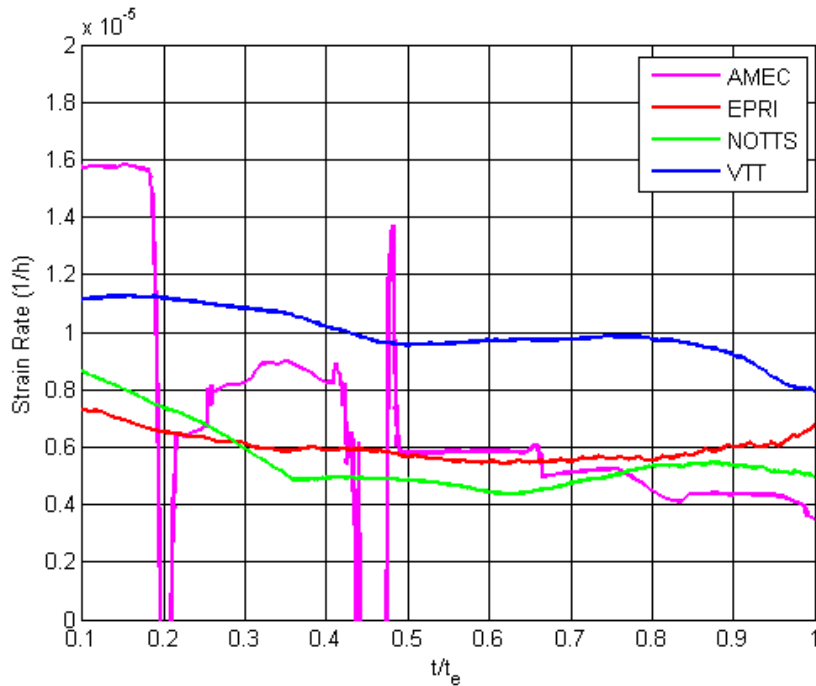


Figure 5: Converted strain rates for all labs at 104 MPa showing a general decreasing trend

DISCUSSION

Data Variation and Applicability

Notable discrepancies between datasets can mainly be observed between the two loading mechanism types, that is dead-weight vs servo. The servo in combination with temperature stability lead to the ability for the load to be kept more consistent. As there is no closed loop load control with the dead-weight loading systems contact with the specimen is maintained but the expansion of the specimen as a result of fluctuations in temperature cannot be accounted for in the displacement signal, hence the larger instability in the displacement traces of the dead-weight machine. In spite of that fluctuation the average strain rates of the rig compare favourably with those of the servo operated machines. Although the data are not plentiful looking at the fluctuation of the test load across all stress levels, there is a clear trend especially when linked to the strain rate plots. The servo-mechanical systems due to their capability for active load control have a more stable signal as can be seen in figure 6

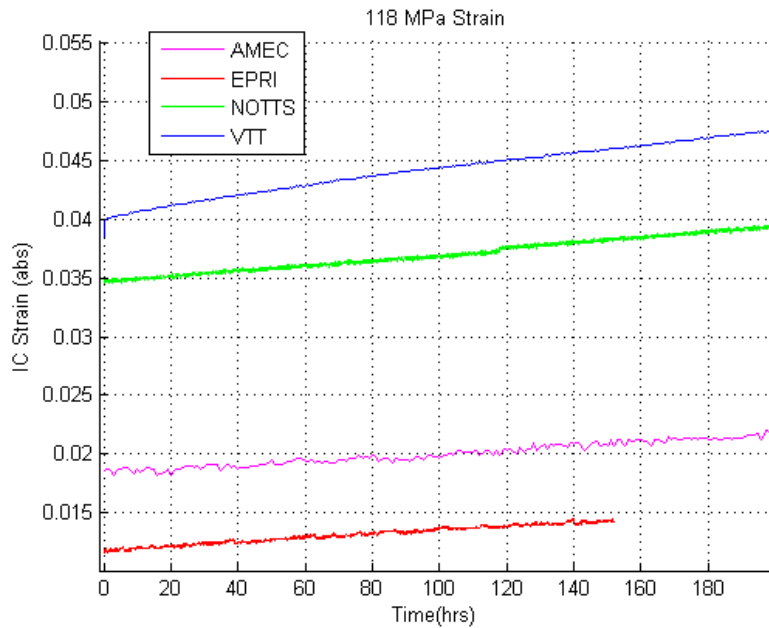


Figure 6: Impression creep traces at 118MPa.

VTT incorporates temperature stability in the order of $\pm 0.3^{\circ}\text{C}$. It has been shown that this temperature accuracy may be surplus to requirements for this particular test. However for materials that may have higher thermal conductivities this level of accuracy may be required.

Requirement for Future Extension

The Impression Monkman Grant relationship has been shown to provide consistency between impression strain data produced in this programme and the strain rate predicted from uniaxial data for the lower bound P91 material BAR257. An analysis of impression strain rates for other materials (preferably power plant steels) against their equivalent uniaxial tests may be useful in determining to what extent this is a general relationship.

The compressive nature of the test causes the secondary creep displacement rates to decrease with time, the effect this has on the strain rates of subsequent loads is assumed to be reductive

however this has not been quantified and so may be a useful area of investigation to be pursued.

CONCLUSIONS

RR testing proved a successful benchmark of four different labs in the experimental impression creep test method, the results indicate that temperature stability has a marked impact on the stability of the creep strain rate, especially if a dead-weight mechanism is used. However, if this stability produces average strain rate comparable to that of more expensive components, there may be an argument to use less costly equipment. The use of simpler loading mechanisms as a low capital cost option for utilities may need further development, due to the frictional effects that arise with the use of such a mechanism. However, for the purposes of precise control and accurate strain rate calculation servo mechanisms are superior.

Acknowledgments

This work is supported by the Engineering and Physical Sciences Research Council (Grant number: EP/G037345/1). The funding is provided through the EPSRC Centre for Doctoral Training in Carbon Capture and Storage and Cleaner Fossil Energy based at the University of Nottingham (ccscfe@nottingham.ac.uk). The work is joint sponsored by the Biomass and Fossil Fuel Research Alliance (BF2RA).

The impression creep tests results reported here were produced by the four collaborating Laboratories: University of Nottingham, UK, Electric Power Research Institute, USA, VTT Technical Research Centre, Finland, and AMEC FW, UK. C. N. C. Dyson and W. Sun would like to acknowledge the support of BF2RA and EPRI, and S. J. Brett would like to acknowledge the support of EPRI via Agreement 10007317.

References

- [1] S. N. G. Chu and J. C. M. Li, "Impression Creep; A New Creep Test," *J. Mater. Sci.*, vol. 12, pp. 2200–2208, 1977.
- [2] T. H. Hyde, W. Sun, and A. A. Becker, "Analysis of the Impression Creep Test Method Using A Rectangular Indenter for Determining the Creep Properties in Welds," *Int. J. Mech. Sci.*, vol. 38, no. 10, pp. 1089–1102, 1995.
- [3] C. Maharaj, J. P. Dear, and a. Morris, "A Review of Methods to Estimate Creep Damage in Low-alloy Steel Power Station Steam Pipes," *Strain*, vol. 45, pp. 316–331, 2009.
- [4] Naveena, V. D. Vijayanand, V. Ganesan, K. Laha, and M. D. Mathew, "Application of Impression Creep Technique for Development of Creep Resistant Austenitic Stainless Steel," *Procedia Eng.*, vol. 55, pp. 585–590, 2013.
- [5] T. H. Hyde, W. Sun, and S. J. Brett, "Some Recommendations on the Standardization of Impression Creep Testing," in *Creep & Fracture in High Temperature Components Design & Life Assessment*, 2009, no. 2.
- [6] B. Cacciapuoti, W. Sun, D. G. McCartney, A. Morris, N. A. Razak, C. M. Davies, J. Hulance, B. Cacciapuoti, W. Sun, D. G. McCartney, A. Morris, N. A. Razak, C. M. Davies, and J. Hulance, "An Evaluation of the Capability of Data Conversion of Impression Creep Test," *Mater. High Temp.*, vol. 3409, no. July, pp. 1–10, 2017.
- [7] T. H. Hyde and W. Sun, "Evaluation of Conversion Relationships for Impression Creep Test at Elevated Temperatures," *Int. J. Press. Vessel. Pip.*, vol. 86, no. 11, pp. 757–763, 2009.
- [8] "Metallic materials - Uniaxial Creep Testing in Tension - Method of test BS EN ISO 204:2009." 2009.
- [9] O. D. Padraic and R. A. Barrett, "A Physically-based Creep Damage Model for Effects of Different Precipitate Types Crossmark," *Mater. Sci. Eng. A*, vol. 682, no. February 2017, pp. 714–722, 2016.
- [10] S. J. Brett, "The Practical Application of Small Scale Sampling and Impression Creep Testing to Grade 91 Components," in *7th International Conference on Advances in Materials Technology for Fossil Power Plants*, 2013.

- [11] W. Bendick, L. Cipolla, J. Gabrel, and J. Hald, “New ECCC Assessment of Creep Rupture Strength for Steel Grade X10CrMoVNb9-1 (Grade 91),” *Int. J. Press. Vessel. Pip.*, vol. 87, no. 6, pp. 304–309, 2010.
- [12] S. J. Brett, “Impression Creep Update,” in *UK High Temperature Power Plant Forum 39th Meeting*, 2015.
- [13] F. Monkman and J. Grant, “An Empirical Relationship Between Rupture Life and Minimum Creep Rate in Creep-rupture Tests,” in *ASTM 56*, 1956, pp. 593–620.

Thanks to the Editor and Referee

1. Grammatical corrections made to line 5 in section 'Introduction'.
2. Errors in punctuation corrected in section 'Introduction'.
3. Grammatical corrections made to line 11 in section 'Introduction'
4. Error in punctuation corrected in section 'Test Set-Up'.
5. Error in formatting corrected in section 'Conversion Relationships'.
6. Clarity of statement made and the addition of grinding tolerances added to section 'Indenter and Specimen'.
7. Punctuation corrections made in section 'Loading Measurement and Control'.
8. Grammatical corrections made to section 'Material and Test Conditions'.
9. Table 2 completed.
10. Grammatical corrections made to section 'Test Rig Descriptions'.
11. New figure added figure 6.

We would like to thank the referee for his kind corrections and suggestions!

Sincerely,

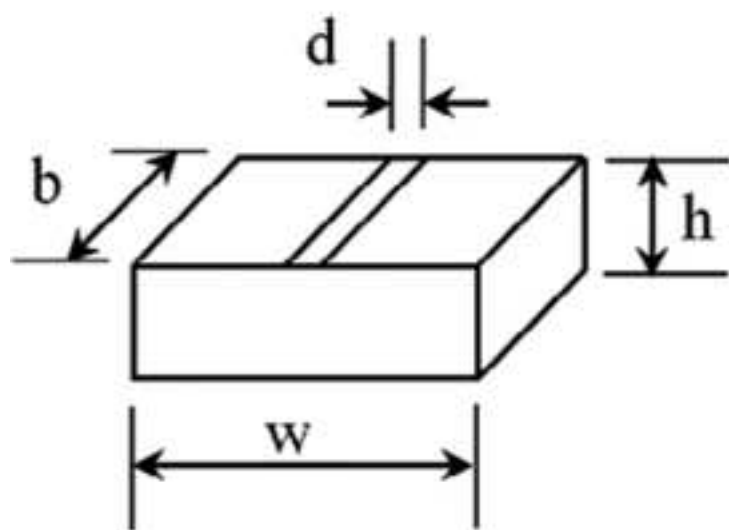
Charles Dyson

BF2RA / CCSCFE EngD Student

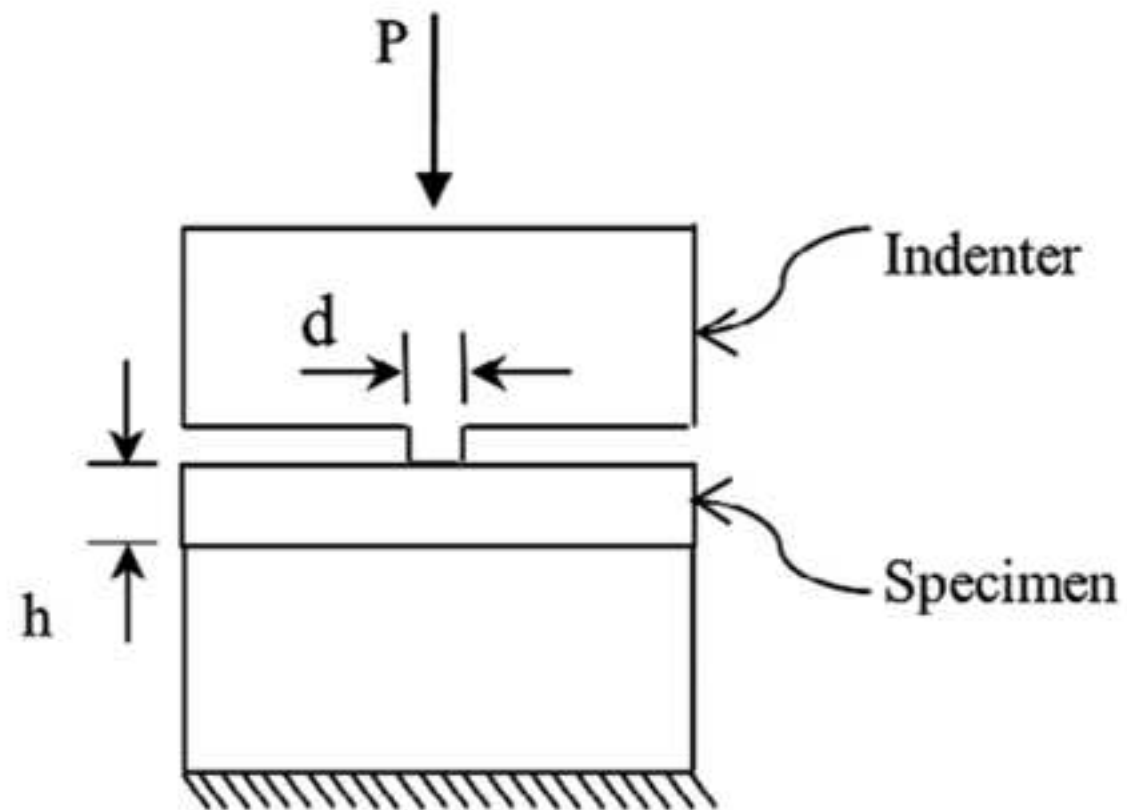
University of Nottingham

ezxcd3@nottingham.ac.uk

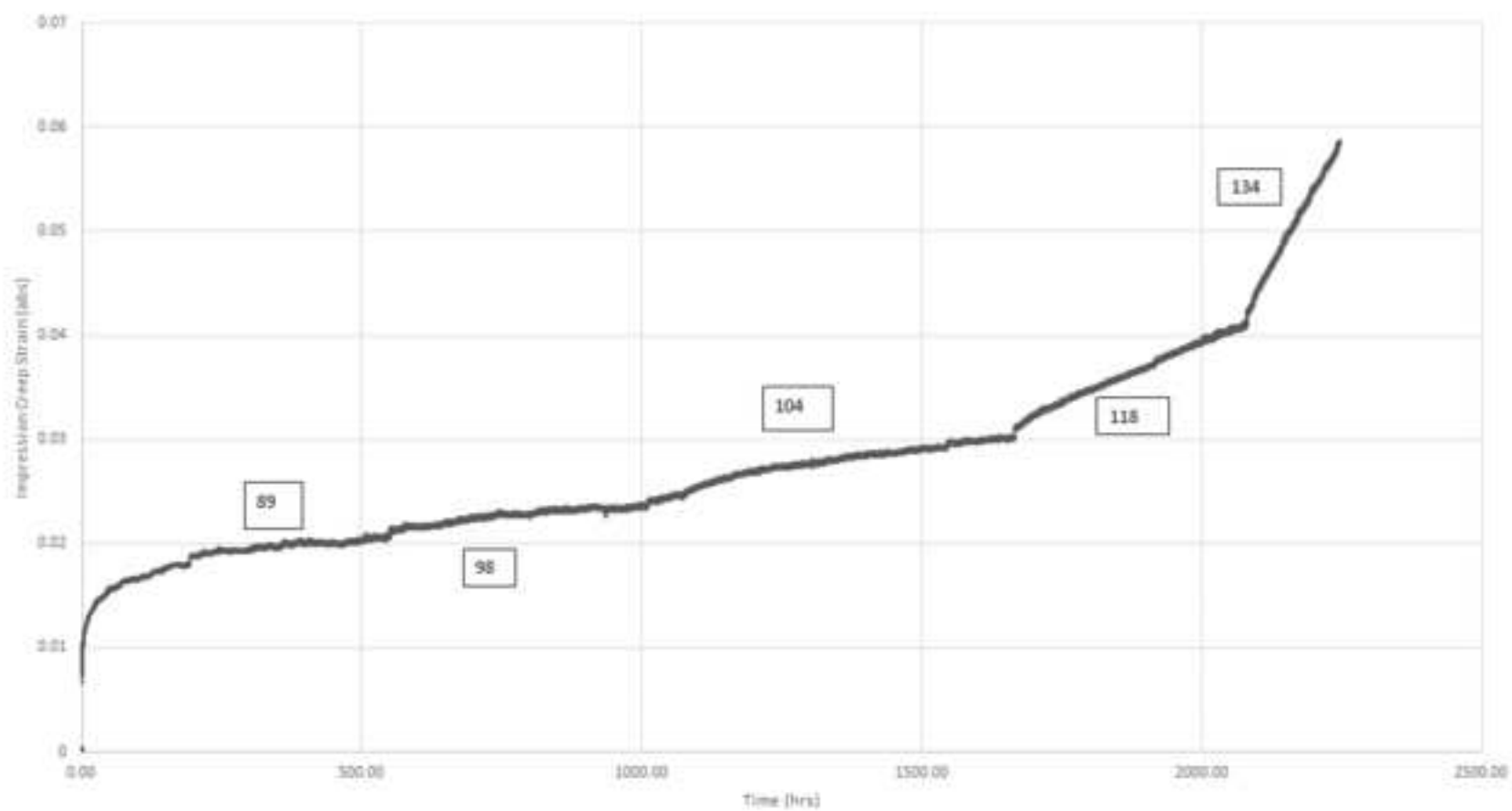
Mobile: +44 7546959066

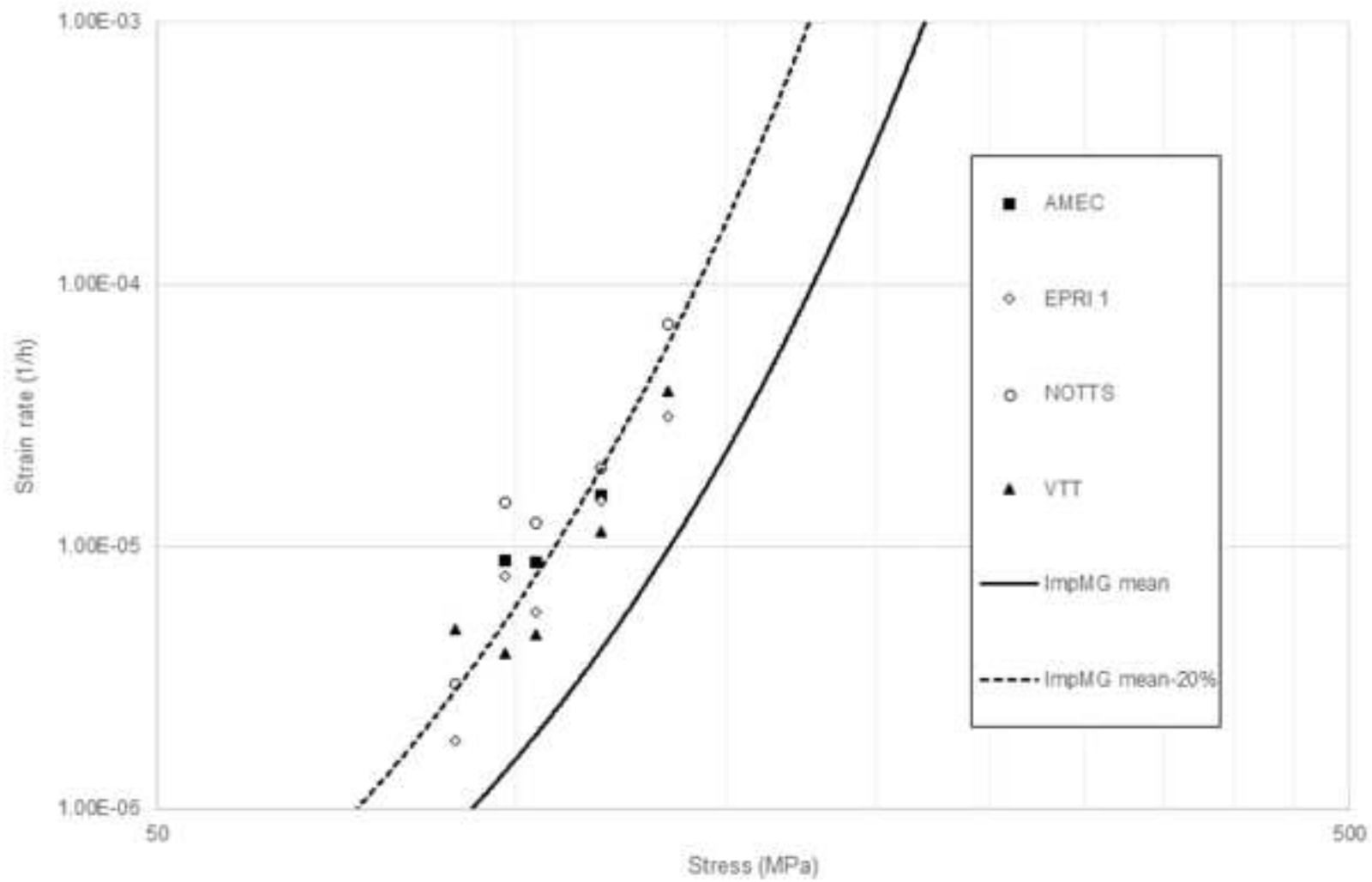


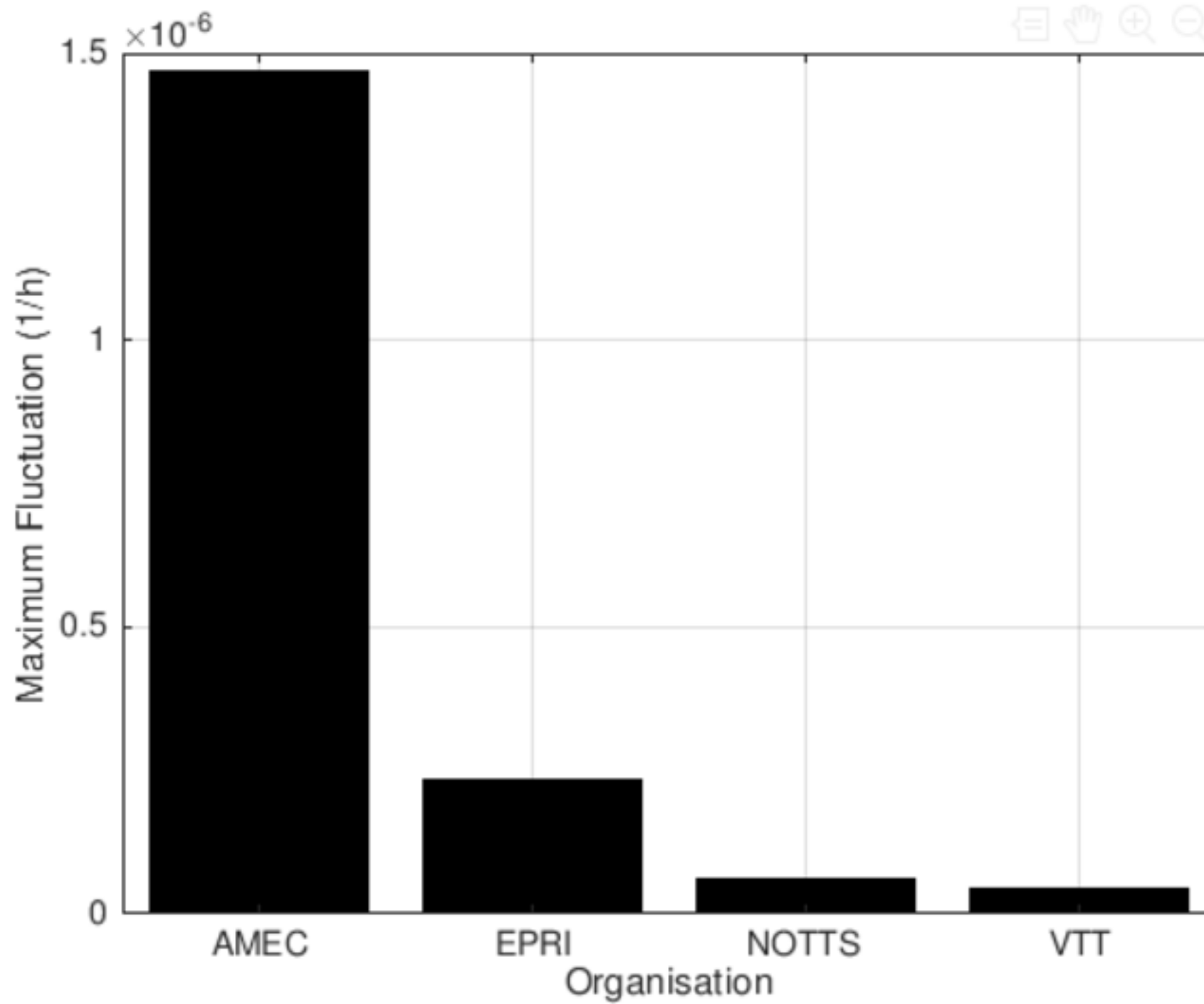
(a)

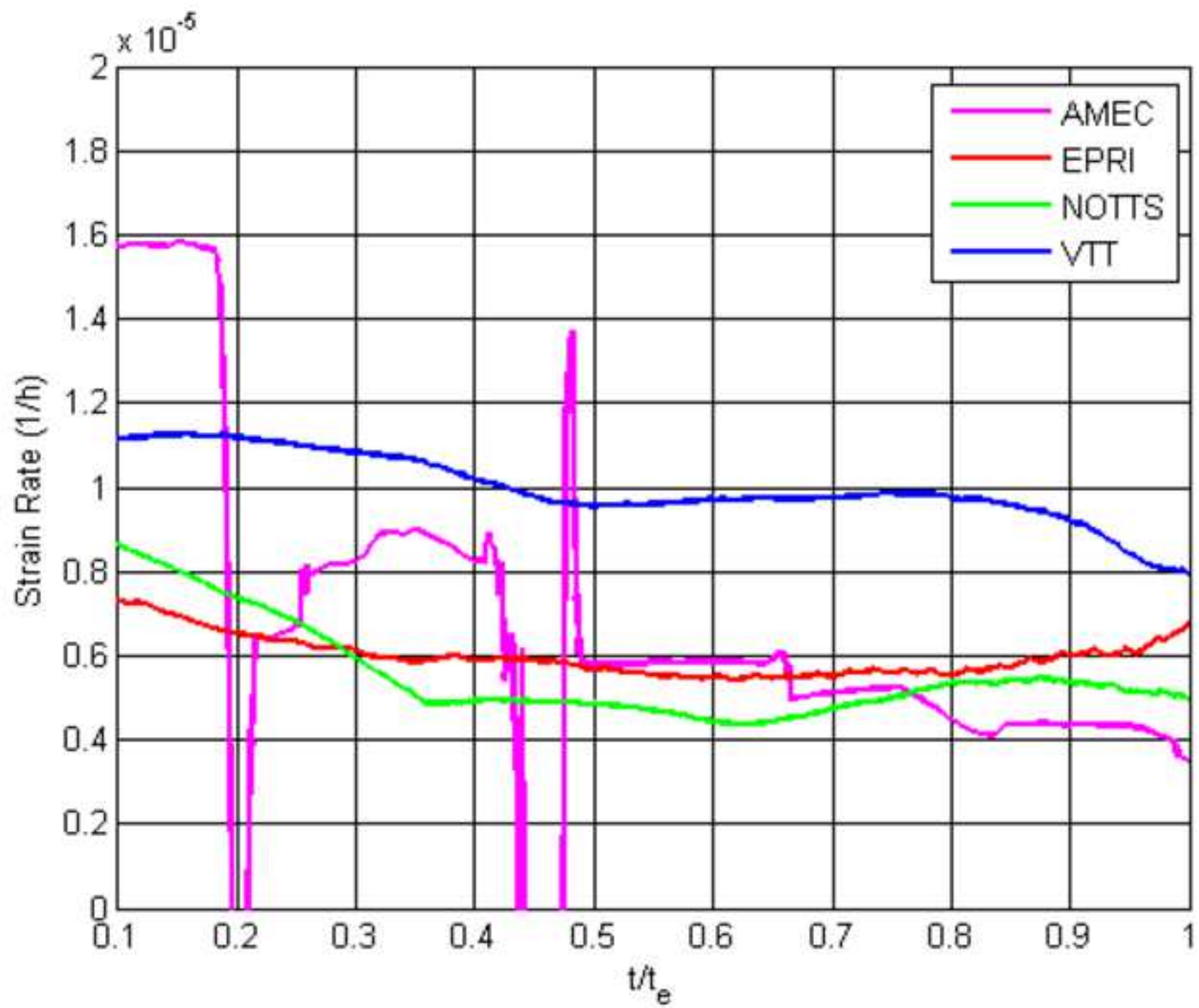


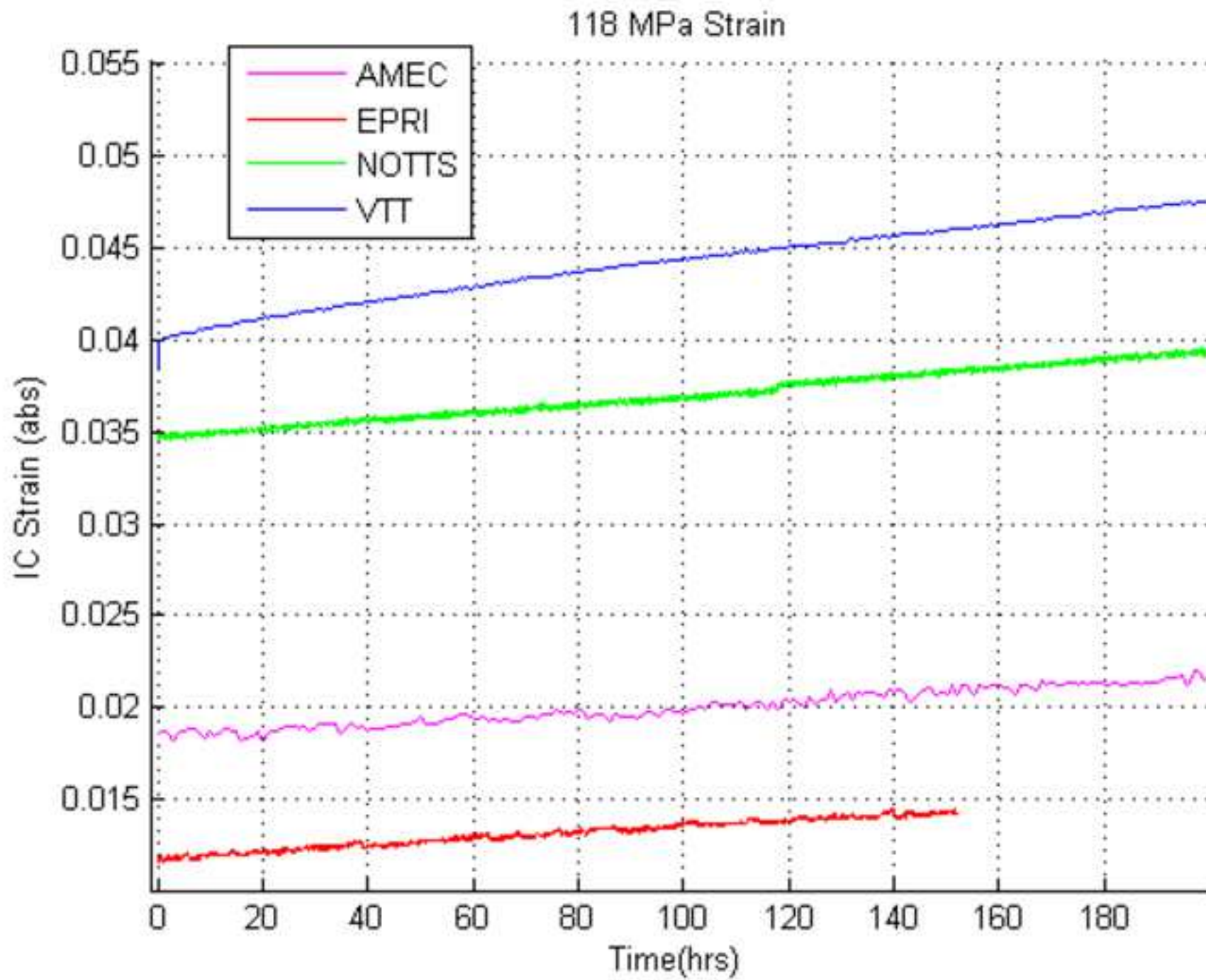
(b)











Impression Creep Test of a P91 Steel: A Round Robin Programme

S.J. Brett¹, C.N.C Dyson^{1*}, D. Purdy², J. Shingledecker², J. Rantala³, J. Eaton-Mckay⁴, W. Sun¹

¹ *Faculty of Engineering, University of Nottingham NG7 2RD, UK*

² *Electric Power Research Institute, Palo Alto, California, USA*

³ *VTT Research Centre FI-02044, Espoo, Finland*

⁴ *AMEC FW, Warrington WA3 6GA, UK*

*Corresponding author: Tel:+44 115 846 7683 email: charles.dyson@nottingham.ac.uk

Impression Creep Test of a P91 Steel: A Round Robin Programme

The process of standardisation of small specimen creep testing techniques, specifically the impression creep test requires the repeatability of the test method. In this study it is accomplished through a round robin programme involving four different labs which have slightly different test set-ups adhering to predefined recommendations stated in previous work. The labs all conducted the same stepped stress test on a reference heat of grade 91 power plant steel and the displacement traces of the tests are analysed to outline the effects of different test set-ups and their efficacies. Main differences are in temperature control and loading application and control.

Keywords: Impression Creep Test; P91; Round Robin Programme

INTRODUCTION

The need for more detailed information in the condition monitoring of power plant components is an ongoing concern which includes high temperature headers, main steam lines, and valve bodies. The use of small specimen creep test methods provides a method to obtain mechanical data from components. The impression creep test method is such a technique, originally starting off as a test using a cylindrical indenter [1] the move to a rectangular indenter loading a square specimen by Hyde et al [2] simplified the technique . It is capable of providing data from in-service components in the form of constant-load displacement rates (converted to the corresponding uniaxial secondary creep strain rates), where specimens are machined from component surface scoop samples. In this instance, strength ranking of components may be conducted and with further development aid in remnant life assessment strategies. In the latter case conversion of the results may be needed as, while in some cases material from the surface of high temperature components may contain the greatest damage [3] in other cases temperature and stress state dependant peak damage may be present below the surface. In scenarios where material is limited, such as

weldments where the separation between metallurgical zones may be small, full-size uniaxial creep testing may not be feasible and so local material characterization may only be possible with small specimen creep tests. In addition to the above requirement, small specimen creep test techniques may be of use in novel alloy development [4] where material quantities and test times are scarce.

The present work is an evaluation of the state of the art procedures involved in testing and is in reference to prior requirements as outlined by Hyde et al [5] who have extensive experience and have conducted hundreds of tests. It has been identified that load stability and control, temperature measurement and control, and displacement measurement are the key variable features in rig design which have a significant impact on test results, particularly displacement signal stability.

IMPRESSION CREEP TEST AND BASIC REQUIREMENTS

Impression Creep Test Using a Rectangular Indenter

Test Set-up

The impression creep testing technique described herein uses rectangular indenters and involves the application of a steady load to a flat-ended indenter, placed on the surface of a specimen, at elevated temperature. The dimensions used across labs in this study are illustrated in Figure 1. $b=h=10$ mm, $w=2.5$, $d=1$

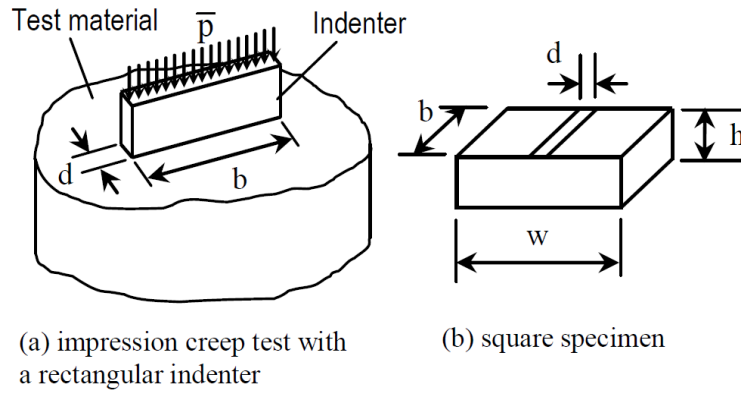


Figure 1: Indenter and specimen dimensions [6]

Conversion Relationships

The displacement-time record obtained from such a test is related to the creep properties of a relatively small volume of material in the immediate vicinity of the indenter. For the rectangular type of indenter, Hyde et al [7] used a reference stress approach to convert the mean pressure under the indenter, \bar{p} , to the corresponding uniaxial stress, σ , i.e.

$$\sigma = \eta \bar{p} \quad (1)$$

and to convert the impression load-direction creep displacement, Δ^c , to the corresponding uniaxial creep strain, ϵ^c , i.e.

$$\epsilon^c = \frac{\Delta^c}{\beta d} \quad (2)$$

where η and β are the conversion parameters (reference parameters) and d is the width of the rectangular indenter, Figure 1(a). Therefore, the secondary creep properties can be obtained from impression creep test data using such conversion relationships. The technique can

produce accurate results when the impression creep deformation occurring during the tests is small, compared with the indenter width or the specimen thickness. This may be done by limiting the secondary creep phase (which has a decreasing displacement rate) by allowing for a secondary creep trace that is approximately linear giving a minimum of a 100h for creep rate calculation, the test lengths are material and stress dependant. The conversion factors however are material independent. They depend on dimension ratios of indenter and specimens if the effect of the impression deformation is neglected. η and β have been determined previously for a practical range of dimensions [2], [7].

Values for η and β are 0.430 and 2.180 [7] respectively for a standard sized specimen, if specimen dimensions are for some reason changed e.g. not enough material could be provided, ref [7] provides details on how to calculate the new values of the parameters.

Basic Requirements

Indenter and Specimen

The indenter must be made of material of significantly higher creep strength than the test material. In the case of fossil power plant pipework (CrMoV, P91) this means the use of nickel superalloys (Waspaloy or Nimonic) or ceramic indenters (Al_2O_3). This is so that creep occurs predominantly in the specimen; i.e. the creep strain rate present in the indenter must be negligible in comparison with the test specimen for the prescribed test conditions. The width of the indenter should also be greater than that of the specimen in order to make sure the whole length of the specimen is indented. A further requirement is that the indenter surfaces are as flat as possible and parallel to each other so as to ensure full contact between the indenter and specimen. Periodic checks between tests must be made on the indenter to make sure that it is flat, including the effects of oxide growth, if not the indenter may be ground so as to be made flat again.

As shown in Figure 1(b), the specimen and indenter dimensions are defined by three ratios; w/d , w/b and h/d . d is the indenter width, w , b and h are the width, length and height of the specimen respectively. The recommended standard dimensions are $w \times b \times h = 10 \times 10 \times 2.5 \text{ mm}$ and $d = 1.0 \text{ mm}$. If material is scarce the height of the specimen can be reduced, as long as conversion requirements are corrected. Or, the standard specimen dimensions can be reduced proportionally e.g. $w \times b \times h = 8 \times 8 \times 2 \text{ mm}$ and $d = 0.8 \text{ mm}$ [7].

Loading, Measurement and Control

Indenter and Specimen Alignment and Load Application

Marking grooves into the specimen before alignment is recommended as guidance for where the indenter blade should sit. This allows for accurate alignment of the indenter to the specimen when placed on the lower loading bar, see Figure 1. Once aligned the specimen must be held in place by the indenter with a load around 10% of the test load so as to secure the specimen before heating. Once the furnace has reached the test temperature the full load may be applied. The applied load should be known to an accuracy of $\pm 1\%$ to agree with requirements in uniaxial creep testing BS EN ISO 204 [8]. In cases where servo mechanical loading is applied there is a requirement for active control,

Displacement Measurement

Displacement measurement can be conducted through the use of water-cooled linear variable displacement transducers (LVDTs) which are connected to the bottom of two extensometers. However, strain gauges or other more advanced methods may be used as long as measuring ranges lie within $\pm 0.2 \text{ mm}$ with an accuracy of 0.5%.

The deformations must be monitored and are recommended to be recorded through signal

conditioning and data logging software. The final displacement recorded by the data logger can be compared to an alternative measurement of the indentation depth for validation.

Optical distance sensing techniques may be used to measure the displacement outside the test furnace.

Temperature Control and Test Environment

The impression creep tests can be performed in air if the test temperatures are within the normal range of operating temperature for the material. Given the compressive contact between the sample and the indenter, oxidation effects on the surface are expected to be minimal even at long test durations.

In the Nottingham creep laboratory, three 0.5mm dia. K type thermocouples are used to control the temperature; however there is no restriction to the use of S type thermocouples. The middle one is close to the specimen and the upper and lower thermocouples are about 25mm away from the specimen, near to the extensometer ridges. These positions may not always be held at the specified temperature due to the heat balance in the furnace. However, experience of many tests, with the temperatures checked by calibrated thermocouples and visual output, has produced a high degree of confidence in using such methods. However, increasing the proximity of the thermocouples to the specimen would not be discouraged. Platinum resistance probes could be used in order to obtain a higher level of accuracy of temperature control or measurement.

BS EN ISO 204 [8] recommends a soak up period of 1 hour for full size uniaxial tests; the same recommendations are then passed on to the impression creep test method before full load is applied.

ROUND ROBIN IMPRESSION CREEP TEST PROGRAMME

Background and Motivation

The testing provides confidence that impression creep is capable of becoming a standardized test technique. In addition, the RR testing is required to show that there is sufficient expertise available to standards organisation bodies when the official standards are ready to be drafted and implemented. It is the aim that a deeper understanding of the test method may be achieved through the use of different set-ups that meet the minimum requirements.

Material and Test Conditions

A variant of P91 power plant steel of the same heat was tested, the material is referred to as BAR257 and has a hardness toward the soft end of the normal range of P91 i.e. 204HV. Its rupture strength shown to be [9], [10] close to 20% below the mean strength value for P91 [11]. The tests done in this Round Robin were stepped stress tests, the load is increased once a secondary creep strain rate is achieved (refer to sect 2.1.2). For this particular series of tests, five stress levels were performed on the same specimen, all at 600⁰C. No previous comparison of this type has been made across all testing laboratories. Loads and their converted stresses can be seen in table 1. Equation (1) is used to make the conversion calculations with $\eta = 0.430$ as the conversion constant. The specimen and indenter dimensions used are those taken from the Basic requirements in Section 2. Nottingham's results can be seen in Figure 2.

Table 1: Impression Creep Stresses

Stress (MPa)	89	98	104	118	134
--------------	----	----	-----	-----	-----

Equipment Specifications

Test Rig Descriptions

Experience at Nottingham has given rise to minimum specifications [5] pertaining to load delivery and sensitivity and the same for temperature. However, there is still scope for variations in rig design as described in table 2 for the different labs. The main purpose of this exercise is to highlight the effects that variations in design have on the indentation traces.

Materials used for the indenters tend to be made of nickel alloys however ceramic indenters may be used provided the sample polishing is increased to a higher level, allowing for less noise in the initial stages of creep, however lower coefficients of thermal expansion would result in increased strain rates in comparison to nickel alloy counterparts which have a similar thermal expansion to P91, it is therefore useful to not only find an indenter of higher creep strength but one with similar expansion properties.

Loading Application

There are two possible loading methods described by the rigs in this programme, 'normal' which involves the indenter blade approaching from above the specimen which is resting on a mount and 'reverse', where the indenter blade is facing upwards and the specimen is loaded onto the blade.

Table 2: Test rig specifications

Organization	Loading Mechanism	Load Accuracy	Indenter Contact Correction	Specimen – indenter Orientation	Heat Delivery	Temperature Control (°C)	Temperature Measurement
AMEC	Dead-weight	10kN	Not required	Normal	Coils built into furnace wall	±0.5	Two k-type thermocouples
EPRI	Servo-mechanical	25kN ±1.25kN	None	Normal	Coils built into furnace wall	±0.5	Three k-type thermocouples
NOTTS	Servo-mechanical	25kN ±1.25kN	None	Normal	Coils built into furnace wall	±0.5	Three k-type thermocouples
VTT	Servo-mechanical	10kN ±0.05kN	Floating indenter system	Reverse	Two flat coils on each loading bar	±0.3	Two R-type thermocouples

Test Results

Converted Minimum Creep Strain Rates

Generally there tends to be good agreement between the labs for the converted average impression creep strain rates (Figure 3). At each stress level within the stepped stress test as in Figure 2 (raw data from each lab is in the appendix) the final 100h of the test are used to calculate the strain rate using a linear regression through the data. Not all step lengths were the same between laboratories, this did not have a marked effect on the results as the 100h window required for calculating strain rates was present across all test data. Other methods were used which yielded results that tended to cluster around the same mean regression through the data points. These included firstly obtaining a plot of the strain rate with time, which is done by taking the slope forward and backward of each data point by either 25h or 50h. Taking the average of the resulting strain rates gave comparable results to those seen in Figure 3 and so the earlier method was used for the plot mainly due to ease of calculation. Figure 3 shows the impression strain rates for each lab compared to the minimum creep strain rate predicted for Grade 91 at mean and mean-20% rupture life values taken from the literature [11] and the Impression Monkman-Grant relationship [12]. The uniaxial formulation of the Monkman-Grant relationship [13] is,

$$C = \varepsilon_{min}^m * t_f \quad (3)$$

where C and m are material constants, ε_{min}^m is the minimum creep strain rate (mmh^{-1}), the equation can be modified to:

$$\text{ICR} = 0.004575 * t_f^{-0.7391} \quad (4)$$

ICR is the impression creep strain rate (mmh^{-1}) and t_f (hrs) is the time to rupture in the conventional uniaxial test. Bar 257 falls in the normal-weak range for P91 and based on the results agrees at the lower stress levels. However at higher stress levels the strain rates deviate. Impression Monkman Grant curves deviate slightly from normal uniaxial curves.

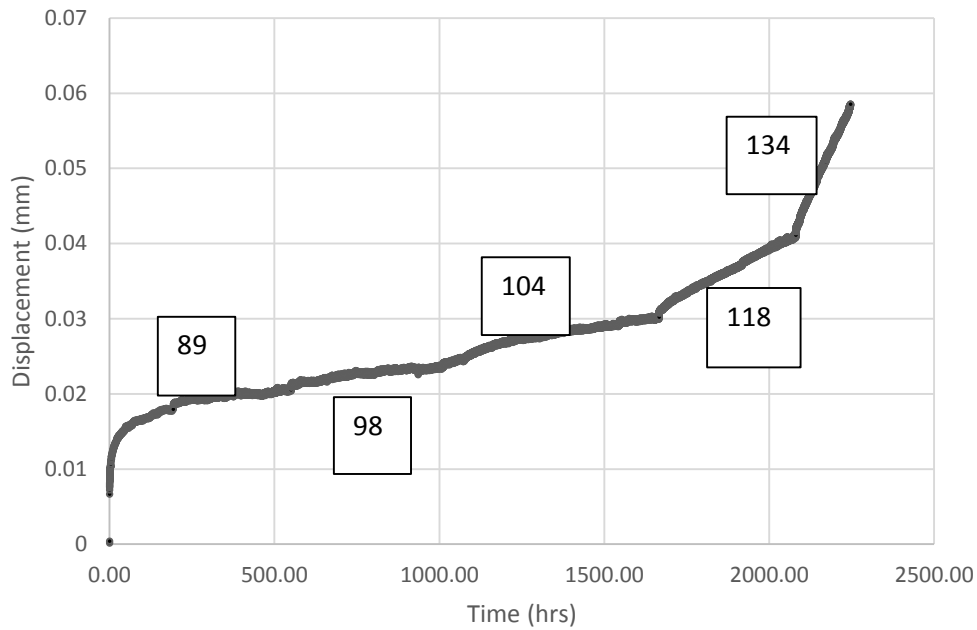


Figure 2: Nottingham stepped stress test results BAR 257 along with loads in MPa at each step

Displacement Rate Variation

For the purposes of the present paper the displacement rate variation will be described as the maximum amplitude in fluctuation of the strain rate signals for each stress level in the stepped stress test. The method used to determine the plot of the strain rate is mentioned above. At each point the strain rate is calculated for points 50h forwards and backwards of that point within the stress level and will be referred to as the 100h strain rate from now on, an example plot for all labs is shown in Figure 5. The maximum amplitude in the signal is determined by detrending the signal and then taking the Fourier transform of the signal to

identify the most prominent amplitude. This is then taken for each stress level and each lab, the averages across stress levels for each lab are compared in Figure 4.

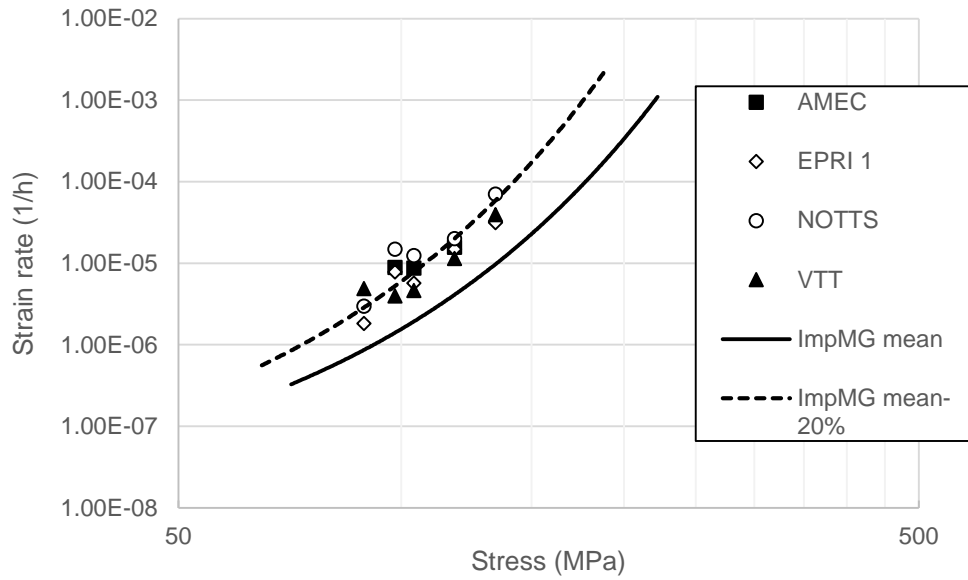


Figure 3: Converted impression strain rates from all labs against the converted strain rate predicted using the ECCC grade 91 mean and mean -20% rupture life [11] and the Impression Monkman Grant relationship

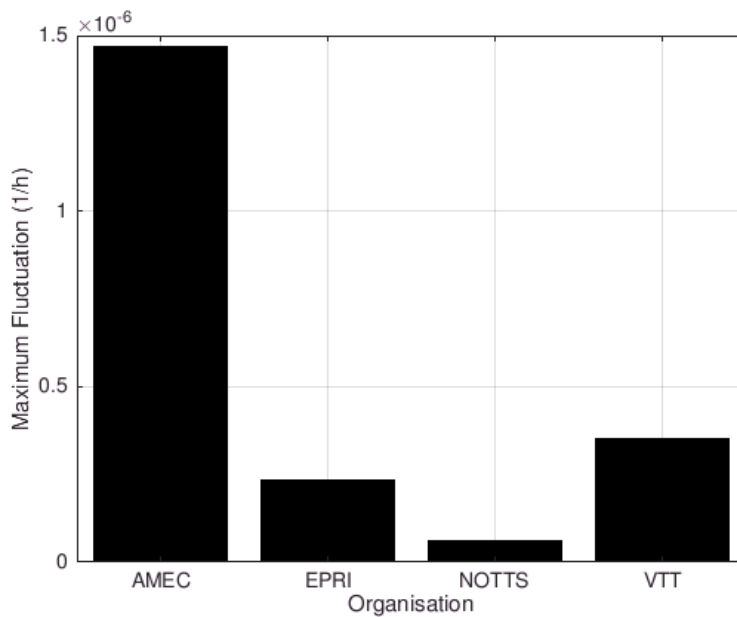


Figure 4: Maximum strain rate fluctuation averaged from all stress levels

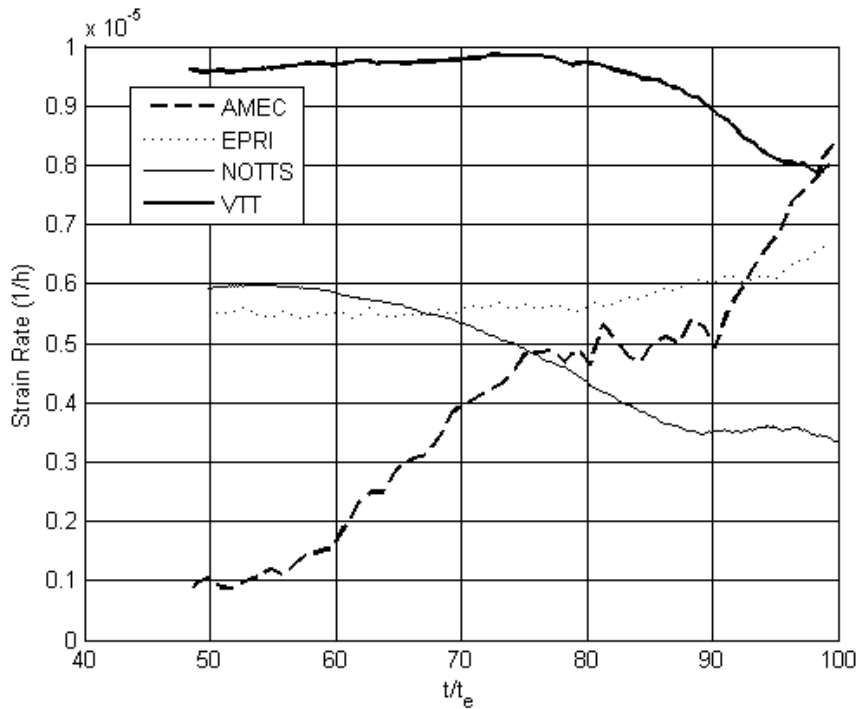


Figure 5: Converted strain rates for all labs at 104 MPa

DISCUSSION

Data Variation and Applicability

Notable discrepancies between datasets can mainly be observed between the two loading mechanism types, that is dead-weight vs servo. The servo in combination with temperature stability lead to the ability for the load to be kept more consistent. As there is no closed loop load control with the dead-weight loading systems contact with the specimen is maintained but the expansion of the specimen as a result of fluctuations in temperature cannot be accounted for in the displacement signal, hence the larger instability in the displacement traces of the dead-weight machine. In spite of that fluctuation the average strain rates of the rig compare favourably with those of the servo operated machines. Although the data are not plentiful looking at the fluctuation of the test load across all stress levels, there is a clear trend

especially when linked to the strain rate plots. The servo-mechanical systems due to their capability for active load control have a more stable signal.

VTT incorporates temperature stability in the order of $\pm 0.3^{\circ}\text{C}$. It has been shown that this temperature accuracy may be surplus to requirements for this particular test. However for materials that may have higher thermal conductivities this level of accuracy may be required.

Requirement for Future Extension

The Impression Monkman Grant relationship has been shown to provide consistency between impression strain data produced in this programme and the strain rate predicted from uniaxial data for the lower bound P91 material BAR257. An analysis of impression strain rates for other materials (preferably power plant steels) against their equivalent uniaxial tests may be useful in determining to what extent this is a general relationship.

The compressive nature of the test causes the secondary creep displacement rates to decrease with time, the effect this has on the strain rates of subsequent loads is assumed to be reductive however this has not been quantified and so may be a useful area of investigation to be pursued.

CONCLUSIONS

RR testing proved a successful benchmark of four different labs in the experimental impression creep test method, the results indicate that temperature stability has a marked impact on the stability of the creep strain rate, especially if a dead-weight mechanism is used. However, if this stability produces average strain rate comparable to that of more expensive

temperature measurement, there may be an argument to use less costly equipment. The use of simpler loading mechanisms as a low capital cost option for utilities may need further development, due to the frictional effects that arise with the use of such a mechanism. However, for the purposes of precise control and accurate strain rate calculation servo mechanisms are superior.

Acknowledgments

This work is supported by the Engineering and Physical Sciences Research Council (Grant number: EP/G037345/1). The funding is provided through the EPSRC Centre for Doctoral Training in Carbon Capture and Storage and Cleaner Fossil Energy based at the University of Nottingham (ccscfe@nottingham.ac.uk). The work is joint sponsored by the Biomass and Fossil Fuel Research Alliance (BF2RA).

The impression creep tests results reported here were produced by the four collaborating Laboratories: University of Nottingham, UK, Electric Power Research Institute, USA, VTT Research Centre, Finland, and AMEC FW, UK. C. N. C. Dyson and W. Sun would like to acknowledge the support of BF2RA, and S. J. Brett would like to acknowledge the support of EPRI via Agreement 10007317.

References

- [1] S. N. G. Chu and J. C. M. Li, "Impression creep; a new creep test," *J. Mater. Sci.*, vol. 12, pp. 2200–2208, 1977.
- [2] T. H. Hyde, W. Sun, and A. A. Becker, "Analysis of the impression creep test method using a rectangular indenter for determining the creep properties in welds," *Int. J. Mech. Sci.*, vol. 38, no. 10, pp. 1089–1102, 1995.
- [3] C. Maharaj, J. P. Dear, and a. Morris, "A review of methods to estimate creep damage in low-alloy steel power station steam pipes," *Strain*, vol. 45, pp. 316–331, 2009.
- [4] Naveena, V. D. Vijayanand, V. Ganesan, K. Laha, and M. D. Mathew, "Application of

- Impression Creep Technique for Development of Creep Resistant Austenitic Stainless Steel,” *Procedia Eng.*, vol. 55, pp. 585–590, 2013.
- [5] T. H. Hyde, W. Sun, and S. J. Brett, “Some Recommendations on the Standardization of Impression Creep Testing,” in *Creep & Fracture in High Temperature Components Design & Life Assessment*, 2009, no. 2.
- [6] T. H. Hyde and W. Sun, “Application of Impression Creep Test Data for the Assessment of Service Exposed Power Plant Components,” *Metall. J.*, vol. 58, pp. 138–145, 2010.
- [7] T. H. Hyde and W. Sun, “Evaluation of conversion relationships for impression creep test at elevated temperatures,” *Int. J. Press. Vessel. Pip.*, vol. 86, no. 11, pp. 757–763, 2009.
- [8] “Metallic materials - Uniaxial creep testing in tension - Method of test BS EN ISO 204:2009.” 2009.
- [9] O. D. Padraic and R. A. Barrett, “A physically-based creep damage model for effects of different precipitate types crossmark,” *Mater. Sci. Eng. A*, vol. 682, no. February 2017, pp. 714–722, 2016.
- [10] S. J. Brett, “The Practical Application of Small Scale Sampling and Impression Creep Testing to Grade 91 Components,” in *7th International Conference on Advances in Materials Technology for Fossil Power Plants*, 2013.
- [11] W. Bendick, L. Cipolla, J. Gabrel, and J. Hald, “New ECCC assessment of creep rupture strength for steel grade X10CrMoVNb9-1 (Grade 91),” *Int. J. Press. Vessel. Pip.*, vol. 87, no. 6, pp. 304–309, 2010.
- [12] S. J. Brett, “Impression Creep Update,” in *UK High Temperature Power Plant Forum 39th Meeting*, 2015.
- [13] F. Monkman and J. Grant, “An empirical relationship between rupture life and minimum creep rate in creep-rupture tests,” in *ASTM 56*, 1956, pp. 593–620.

Impression Creep Test of a P91 Steel: A Round Robin Programme

S.J. Brett¹, C.N.C Dyson^{1*}, D. Purdy², J. Shingledecker², J. Rantala³, J. Eaton-Mckay⁴, W. Sun¹

¹ *Faculty of Engineering, University of Nottingham NG7 2RD, UK*

² *Electric Power Research Institute, Palo Alto, California, USA*

³ *VTT Technical Research Centre FI-02044, Espoo, Finland*

⁴ *AMEC FW, Warrington WA3 6GA, UK*

*Corresponding author: Tel:+44 115 846 7683 email: ezxcd3@nottingham.ac.uk

Impression Creep Test of a P91 Steel: A Round Robin Programme

Abstract:

The process of standardisation of small specimen creep testing techniques, specifically the impression creep test requires the repeatability of the test method. In this study it is accomplished through a round robin programme involving four different labs which have slightly different test set-ups adhering to predefined recommendations stated in previous work. The labs all conducted the same stepped stress test on a reference heat of grade 91 power plant steel and the displacement traces of the tests are analysed to outline the effects of different test set-ups and their efficacies. Main differences are in temperature control and loading application and control.

Keywords: Impression Creep Test; P91; Round Robin Programme

INTRODUCTION

The need for more detailed information in the condition monitoring of power plant components is an ongoing concern which includes high temperature headers, main steam lines, and valve bodies. The use of small specimen creep test methods provides a method to obtain mechanical data from components. The impression creep test method is such a technique, originally performed using a cylindrical indenter [1], and later using a rectangular indenter loading a square specimen from which a mechanics based interpretation technique was developed [2]. It is capable of providing data from in-service components in the form of constant-load displacement rates (converted to the corresponding uniaxial secondary creep strain rates), where specimens are machined from component surface scoop samples. In this instance, strength ranking of components may be conducted and with further development aid in remnant life assessment strategies. In the latter case, conversion of the results may be needed. While in some cases material from the surface of high temperature components may contain the greatest damage [3] in other cases temperature and stress state dependant peak

damage may be present below the surface. In scenarios where material is limited, such as weldments where the separation between metallurgical zones may be small, full-size uniaxial creep testing may not be feasible and so local material characterization may only be possible with small specimen creep tests. In addition to the above requirement, small specimen creep test techniques may be of use in novel alloy development [4] where material quantities and test times are scarce.

The present work is an evaluation of the state of the art procedures involved in testing and is in reference to prior requirements as outlined by Hyde et al [5] who have extensive experience and have conducted hundreds of tests. It has been identified that load stability and control, temperature measurement and control, and displacement measurement are the key variable features in rig design which have a significant impact on test results, particularly displacement signal stability.

IMPRESSION CREEP TEST AND BASIC REQUIREMENTS

Impression Creep Test Using a Rectangular Indenter

Test Set-up

The impression creep testing technique described herein uses rectangular indenters and involves the application of a steady load to a flat-ended indenter, placed on the surface of a specimen, at elevated temperature. The dimensions used across labs in this study are illustrated in Figure 1. $b=w=10$ mm, $h=2.5$ and $d=1$.

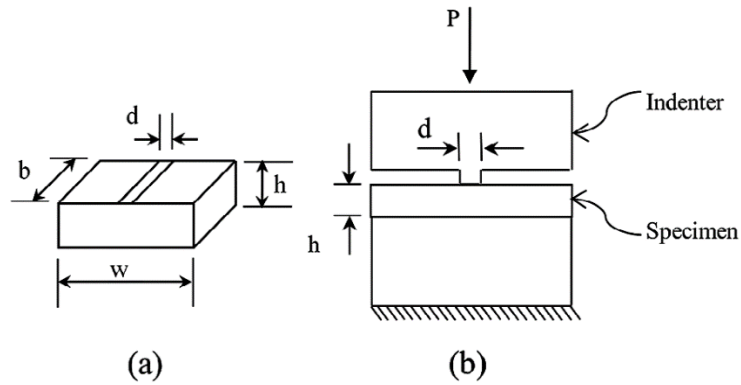


Figure 1: Indenter and specimen dimensions [6]

Conversion Relationships

The displacement-time record obtained from such a test is related to the creep properties of a relatively small volume of material in the immediate vicinity of the indenter. For the rectangular type of indenter, Hyde et al [7] used a reference stress approach to convert the mean pressure under the indenter, \bar{p} , to the corresponding uniaxial stress, σ , i.e.

$$\sigma = \eta \bar{p} \quad (1)$$

and to convert the impression load-direction creep displacement, Δ^c , to the corresponding uniaxial creep strain, ϵ^c , i.e.

$$\epsilon^c = \frac{\Delta^c}{\beta d} \quad (2)$$

where η and β are the conversion parameters (reference parameters) and d is the width of the rectangular indenter, Figure 1(a). Therefore, the secondary creep properties can be obtained from impression creep test data using such conversion relationships. The technique can

produce accurate results when the impression creep deformation occurring during the tests is small, compared with the indenter width or the specimen thickness. This may be done by limiting the secondary creep phase (which has a decreasing displacement rate) by allowing for a secondary creep trace that is approximately linear giving a minimum of a 100h for creep rate calculation, the test lengths are material and stress dependant. The conversion factors however are material independent. They depend on dimension ratios of indenter and specimens if the effect of the indenter deformation is neglected. η and β have been determined previously for a practical range of dimensions [2], [7].

Values for η and β are 0.430 and 2.180 [7] respectively for a standard sized specimen, if specimen dimensions are for some reason changed e.g. not enough material could be provided, ref [7] provides details on how to calculate the new values of the parameters.

Basic Requirements

Indenter and Specimen

The indenter must be made of material of significantly higher creep strength than the test material. In the case of fossil power plant pipework (CrMoV, P91) this means the use of nickel superalloys (Waspaloy or Nimonic) or ceramic indenters (Al_2O_3). This is so that creep occurs predominantly in the specimen; i.e. the creep strain rate present in the indenter must be negligible in comparison with the test specimen for the prescribed test conditions. The width of the indenter should also be greater than that of the specimen in order to make sure the whole length of the specimen is indented. A further requirement is that the indenter should be ground so as to be parallel with the flat surface of the specimen. Periodic checks between tests must be made on the indenter to make sure that it is flat, including the effects of oxide growth, if not the indenter may be ground so as to be made flat again, polishing of the surfaces to a recommended 200grit with a tolerance of $\pm 0.02\text{mm}$.

As shown in Figure 1(b), the specimen and indenter dimensions are defined by three ratios; w/d , w/b and h/d . d is the indenter width, w , b and h are the width, length and height of the specimen respectively. The recommended standard dimensions are $w \times b \times h = 10 \times 10 \times 2.5 \text{ mm}$ and $d = 1.0 \text{ mm}$. If material is scarce the height of the specimen can be reduced, as long as conversion requirements are corrected. Or, the standard specimen dimensions can be reduced proportionally e.g. $w \times b \times h = 8 \times 8 \times 2 \text{ mm}$ and $d = 0.8 \text{ mm}$ [7].

Loading, Measurement and Control

Indenter and Specimen Alignment and Load Application

Marking grooves into the specimen before alignment is recommended as guidance for where the indenter blade should sit. This allows for accurate alignment of the indenter to the specimen when placed on the lower loading bar, see Figure 1. Once aligned the specimen must be held in place by the indenter with a load around 10% of the test load so as to secure the specimen before heating. Once the furnace has reached the test temperature the full load may be applied. The applied load should be known to an accuracy of $\pm 1\%$ to agree with requirements in uniaxial creep testing BS EN ISO 204 [8]. In cases where servo mechanical loading is applied there is a requirement for active control.

Displacement Measurement

Displacement measurement can be conducted through the use of water-cooled linear variable displacement transducers (LVDTs) which are connected to the bottom of two extensometers. However, strain gauges or other more advanced methods may be used as long as measuring ranges lie within $\pm 0.2 \text{ mm}$ with an accuracy of 0.5%.

The deformations must be monitored and are recommended to be recorded through signal

conditioning and data logging software. The final displacement recorded by the data logger can be compared to an alternative measurement of the indentation depth for validation.

Temperature Control and Test Environment

The impression creep tests can be performed in air if the test temperatures are within the normal range of operating temperature for the material. Given the compressive contact between the sample and the indenter, oxidation effects on the surface are expected to be minimal even at long test durations.

In the Nottingham creep laboratory, three 0.5mm dia. K type thermocouples are used to control the temperature; however there is no restriction to the use of S type thermocouples. The middle one is close to the specimen and the upper and lower thermocouples are about 25mm away from the specimen, near to the extensometer ridges. These positions may not always be held at the specified temperature due to the heat balance in the furnace. However, experience of many tests, with the temperatures checked by calibrated thermocouples and visual output, has produced a high degree of confidence in using such methods. However, increasing the proximity of the thermocouples to the specimen would not be discouraged. Platinum resistance probes could be used in order to obtain a higher level of accuracy of temperature control or measurement.

BS EN ISO 204 [8] recommends a soak up period of 1 hour for full size uniaxial tests; the same recommendations are then passed on to the impression creep test method before full load is applied.

ROUND ROBIN IMPRESSION CREEP TEST PROGRAMME

Background and Motivation

The testing provides confidence that impression creep is capable of becoming a standardized test technique. In addition, the RR testing is required to show that there is sufficient expertise available to standards organisation bodies when the official standards are ready to be drafted and implemented. It is the aim that a deeper understanding of the test method may be achieved through the use of different set-ups that meet the minimum requirements.

Material and Test Conditions

A variant of P91 power plant steel of the same heat was tested, the material is referred to as BAR257 and has a hardness toward the soft end of the normal range of P91 i.e. 204HV. Its rupture strength shown to be [9], [10] close to 20% below the mean strength value for P91 [11]. The tests done in this Round Robin were stepped stress tests, the load is increased once a sufficiently low secondary creep strain rate is achieved (refer to sect 2.1.2). For this particular series of tests, five stress levels were performed on the same specimen, all at 600°C. No previous comparison of this type has been made across all testing laboratories. Loads and their converted stresses can be seen in table 1. Equation (1) is used to make the conversion calculations with $\eta = 0.430$ as the conversion constant. The specimen and indenter dimensions used are those taken from the Basic requirements in Section 2. Nottingham's results can be seen in Figure 2.

Table 1: Impression Creep Stresses

Stress (MPa)	89	98	104	118	134
--------------	----	----	-----	-----	-----

Equipment Specifications

Test Rig Descriptions

Experience at Nottingham has given rise to minimum specifications [5] pertaining to load delivery and sensitivity and the same for temperature. However, there is still scope for variations in rig design as described in table 2 for the different labs. The main purpose of this exercise is to highlight the effects that variations in design have on the indentation traces.

Materials used for the indenters can be made of nickel based super alloys however ceramic indenters may be used provided the sample polishing is increased to a higher level, allowing for less noise in the initial stages of creep. However lower coefficients of thermal expansion would result in increased strain rates in comparison to nickel alloy counterparts which have a similar thermal expansion to P91. It is therefore useful to not only find an indenter of higher creep strength but one with similar thermal expansion properties.

Loading Application

There are two possible loading methods described by the rigs in this programme, 'normal' which involves the indenter blade approaching from above the specimen which is resting on a mount and 'reverse', where the indenter blade is facing upwards and the specimen is loaded onto the blade.

Table 2: Test Rig Specifications

Organization	Loading Mechanism	Load Accuracy	Indenter Contact Correction	Specimen – indenter Orientation	Heat Delivery	Temperature Control (°C)	Temperature Measurement
AMEC	Dead-weight	10kN ±0.05N	Not required	Normal	Coils built into furnace wall	±0.5	Two k-type thermocouples
EPRI	Servo-mechanical	25kN ±1.25N	None	Normal	Coils built into furnace wall	±0.5	Three k-type thermocouples
NOTTS	Servo-mechanical	25kN ±1.25N	None	Normal	Coils built into furnace wall	±0.5	Three k-type thermocouples
VTT	Servo-mechanical	10kN ±0.05N	Floating indenter system	Reverse	Two flat coils on each loading bar	±0.3	Two R-type thermocouples

Test Results

Converted Minimum Creep Strain Rates

Generally there tends to be good agreement between the labs for the converted average impression creep strain rates (Figure 3). At each stress level within the stepped stress test as in Figure 2 (raw data from each lab is in the appendix) the final 100h of the test are used to calculate the strain rate using a linear regression through the data. Not all step lengths were the same between laboratories, this did not have a marked effect on the results as the 100h window required for calculating strain rates was present across all test data. Other methods were used which yielded results that tended to cluster around the same mean regression through the data points. These included firstly obtaining a plot of the strain rate with time, which is done by taking the slope forward and backward of each data point by either 25h or 50h. Taking the average of the resulting strain rates gave comparable results to those seen in Figure 3 and so the earlier method was used for the plot mainly due to ease of calculation. Figure 3 shows the impression strain rates for each lab compared to the minimum creep strain rate predicted for Grade 91 at mean and mean-20% rupture life values taken from the literature [11] and the Impression Monkman-Grant relationship [12]. The uniaxial formulation of the Monkman-Grant relationship [13] is,

$$C = \dot{\epsilon}_{min}^C * t_f \quad (3)$$

where C and m are material constants, $\dot{\epsilon}_{min}^C$ is the minimum creep strain rate (h^{-1}), the equation can be modified to:

$$ICR = 0.004575 * t_f^{-0.7391} \quad (4)$$

ICR is the impression creep strain rate (mmh^{-1}) and t_f (hrs) is the time to rupture in the conventional uniaxial test. Bar 257 falls in the normal-weak range for P91 and based on the results agrees at the lower stress levels. However at higher stress levels the strain rates deviate. Impression Monkman Grant curves deviate slightly from normal uniaxial curves.

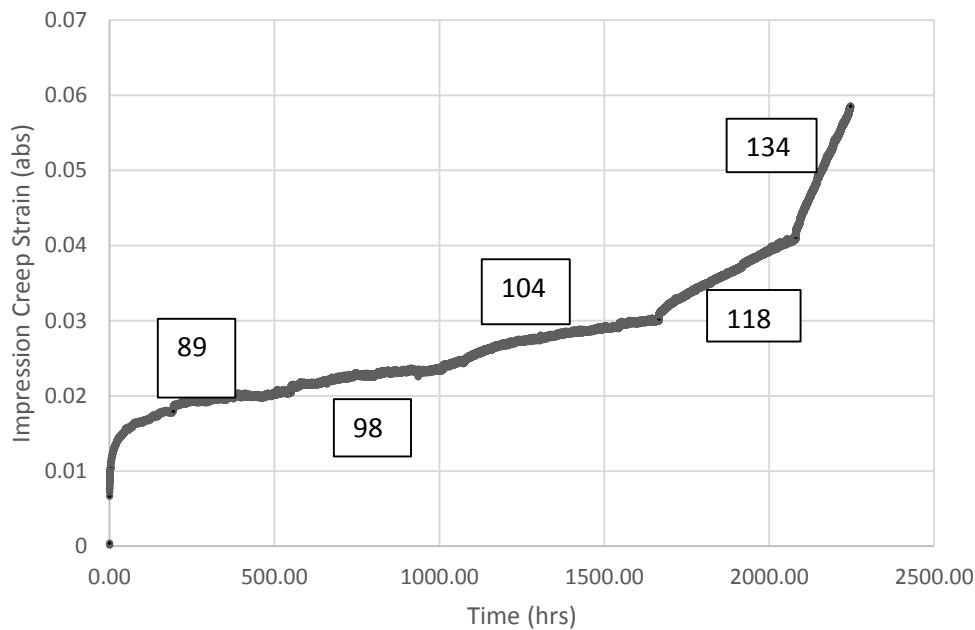


Figure 2: Nottingham stepped stress test results BAR 257 along with loads in MPa at each step

Displacement Rate Variation

For the purposes of the present paper the displacement rate variation will be described as the maximum amplitude in fluctuation of the strain rate signals for each stress level in the stepped stress test. The method used to determine the plot of the strain rate is mentioned above. At each point the strain rate is calculated for points 50h forwards and backwards of that point within the stress level and will be referred to as the 100h strain rate from now on, an example plot for all labs is shown in Figure 5. The maximum amplitude in the signal is determined by detrending the signal and then taking the Fourier transform of the signal to

identify the most prominent amplitude. This is then taken for each stress level and each lab, the averages across stress levels for each lab are compared in Figure 4.

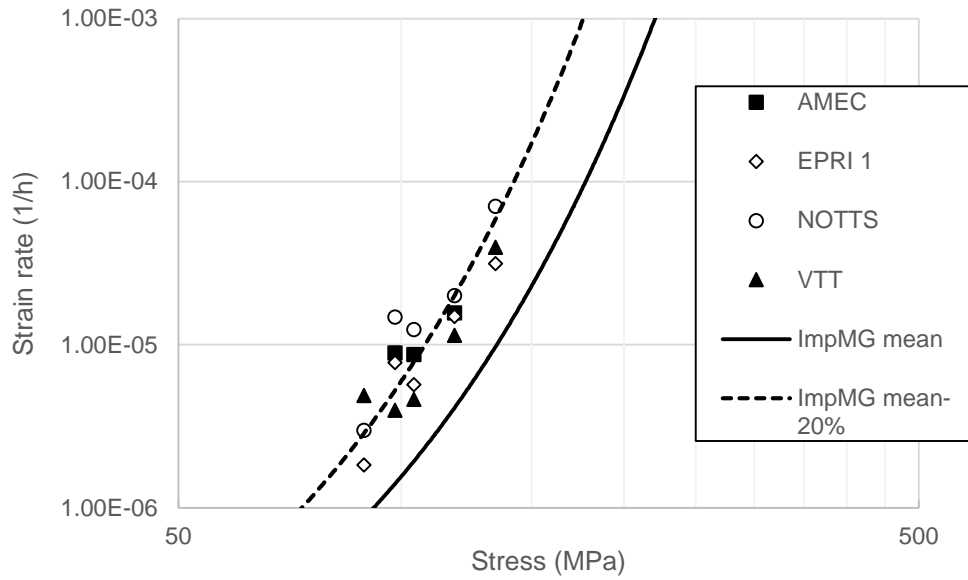


Figure 3: Converted impression strain rates from all labs against the converted strain rate predicted using the ECCC grade 91 mean and mean -20% rupture life [11] and the Impression Monkman Grant relationship

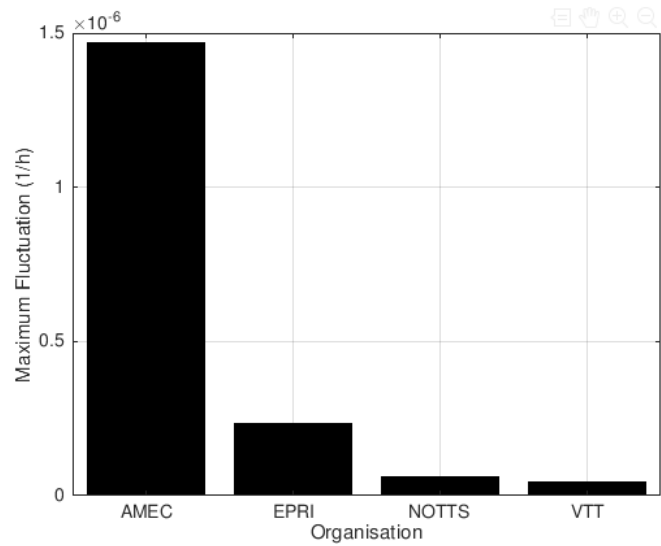


Figure 4: Maximum strain rate fluctuation averaged from all stress levels

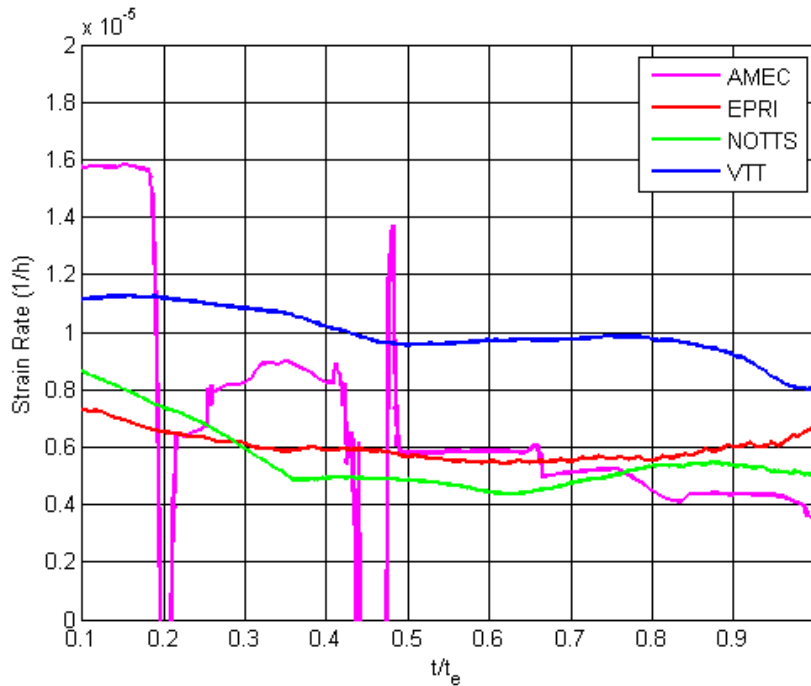


Figure 5: Converted strain rates for all labs at 104 MPa showing a general decreasing trend

DISCUSSION

Data Variation and Applicability

Notable discrepancies between datasets can mainly be observed between the two loading mechanism types, that is dead-weight vs servo. The servo in combination with temperature stability lead to the ability for the load to be kept more consistent. As there is no closed loop load control with the dead-weight loading systems contact with the specimen is maintained but the expansion of the specimen as a result of fluctuations in temperature cannot be accounted for in the displacement signal, hence the larger instability in the displacement traces of the dead-weight machine. In spite of that fluctuation the average strain rates of the rig compare favourably with those of the servo operated machines. Although the data are not plentiful looking at the fluctuation of the test load across all stress levels, there is a clear trend especially when linked to the strain rate plots. The servo-mechanical systems due to their capability for active load control have a more stable signal as can be seen in figure 6

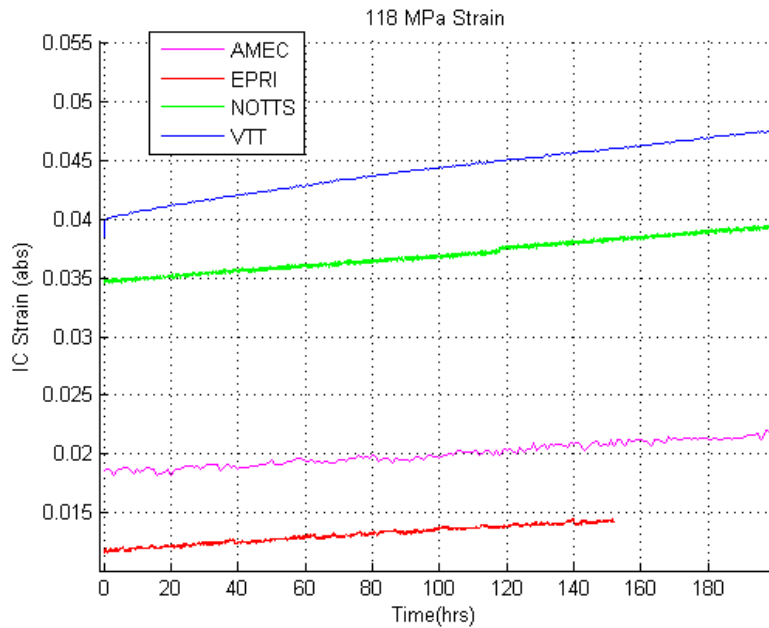


Figure 6: Impression creep traces at 118MPa.

VTT incorporates temperature stability in the order of $\pm 0.3^{\circ}\text{C}$. It has been shown that this temperature accuracy may be surplus to requirements for this particular test. However for materials that may have higher thermal conductivities this level of accuracy may be required.

Requirement for Future Extension

The Impression Monkman Grant relationship has been shown to provide consistency between impression strain data produced in this programme and the strain rate predicted from uniaxial data for the lower bound P91 material BAR257. An analysis of impression strain rates for other materials (preferably power plant steels) against their equivalent uniaxial tests may be useful in determining to what extent this is a general relationship.

The compressive nature of the test causes the secondary creep displacement rates to decrease with time, the effect this has on the strain rates of subsequent loads is assumed to be reductive

however this has not been quantified and so may be a useful area of investigation to be pursued.

CONCLUSIONS

RR testing proved a successful benchmark of four different labs in the experimental impression creep test method, the results indicate that temperature stability has a marked impact on the stability of the creep strain rate, especially if a dead-weight mechanism is used. However, if this stability produces average strain rate comparable to that of more expensive components, there may be an argument to use less costly equipment. The use of simpler loading mechanisms as a low capital cost option for utilities may need further development, due to the frictional effects that arise with the use of such a mechanism. However, for the purposes of precise control and accurate strain rate calculation servo mechanisms are superior.

Acknowledgments

This work is supported by the Engineering and Physical Sciences Research Council (Grant number: EP/G037345/1). The funding is provided through the EPSRC Centre for Doctoral Training in Carbon Capture and Storage and Cleaner Fossil Energy based at the University of Nottingham (ccscfe@nottingham.ac.uk). The work is joint sponsored by the Biomass and Fossil Fuel Research Alliance (BF2RA).

The impression creep tests results reported here were produced by the four collaborating Laboratories: University of Nottingham, UK, Electric Power Research Institute, USA, VTT Technical Research Centre, Finland, and AMEC FW, UK. C. N. C. Dyson and W. Sun would like to acknowledge the support of BF2RA and EPRI, and S. J. Brett would like to acknowledge the support of EPRI via Agreement 10007317.

References

- [1] S. N. G. Chu and J. C. M. Li, "Impression Creep; A New Creep Test," *J. Mater. Sci.*, vol. 12, pp. 2200–2208, 1977.
- [2] T. H. Hyde, W. Sun, and A. A. Becker, "Analysis of the Impression Creep Test Method Using A Rectangular Indenter for Determining the Creep Properties in Welds," *Int. J. Mech. Sci.*, vol. 38, no. 10, pp. 1089–1102, 1995.
- [3] C. Maharaj, J. P. Dear, and a. Morris, "A Review of Methods to Estimate Creep Damage in Low-alloy Steel Power Station Steam Pipes," *Strain*, vol. 45, pp. 316–331, 2009.
- [4] Naveena, V. D. Vijayanand, V. Ganesan, K. Laha, and M. D. Mathew, "Application of Impression Creep Technique for Development of Creep Resistant Austenitic Stainless Steel," *Procedia Eng.*, vol. 55, pp. 585–590, 2013.
- [5] T. H. Hyde, W. Sun, and S. J. Brett, "Some Recommendations on the Standardization of Impression Creep Testing," in *Creep & Fracture in High Temperature Components Design & Life Assessment*, 2009, no. 2.
- [6] B. Cacciapuoti, W. Sun, D. G. McCartney, A. Morris, N. A. Razak, C. M. Davies, J. Hulance, B. Cacciapuoti, W. Sun, D. G. McCartney, A. Morris, N. A. Razak, C. M. Davies, and J. Hulance, "An Evaluation of the Capability of Data Conversion of Impression Creep Test," *Mater. High Temp.*, vol. 3409, no. July, pp. 1–10, 2017.
- [7] T. H. Hyde and W. Sun, "Evaluation of Conversion Relationships for Impression Creep Test at Elevated Temperatures," *Int. J. Press. Vessel. Pip.*, vol. 86, no. 11, pp. 757–763, 2009.
- [8] "Metallic materials - Uniaxial Creep Testing in Tension - Method of test BS EN ISO 204:2009." 2009.
- [9] O. D. Padraic and R. A. Barrett, "A Physically-based Creep Damage Model for Effects of Different Precipitate Types Crossmark," *Mater. Sci. Eng. A*, vol. 682, no. February 2017, pp. 714–722, 2016.
- [10] S. J. Brett, "The Practical Application of Small Scale Sampling and Impression Creep Testing to Grade 91 Components," in *7th International Conference on Advances in Materials Technology for Fossil Power Plants*, 2013.

- [11] W. Bendick, L. Cipolla, J. Gabrel, and J. Hald, “New ECCC Assessment of Creep Rupture Strength for Steel Grade X10CrMoVNb9-1 (Grade 91),” *Int. J. Press. Vessel. Pip.*, vol. 87, no. 6, pp. 304–309, 2010.
- [12] S. J. Brett, “Impression Creep Update,” in *UK High Temperature Power Plant Forum 39th Meeting*, 2015.
- [13] F. Monkman and J. Grant, “An Empirical Relationship Between Rupture Life and Minimum Creep Rate in Creep-rupture Tests,” in *ASTM 56*, 1956, pp. 593–620.